Faculty of Aerospace Engineering

The Role of Motion Feedback in Manual Preview Tracking Tasks

J. Morais Almeida

August 24, 2016

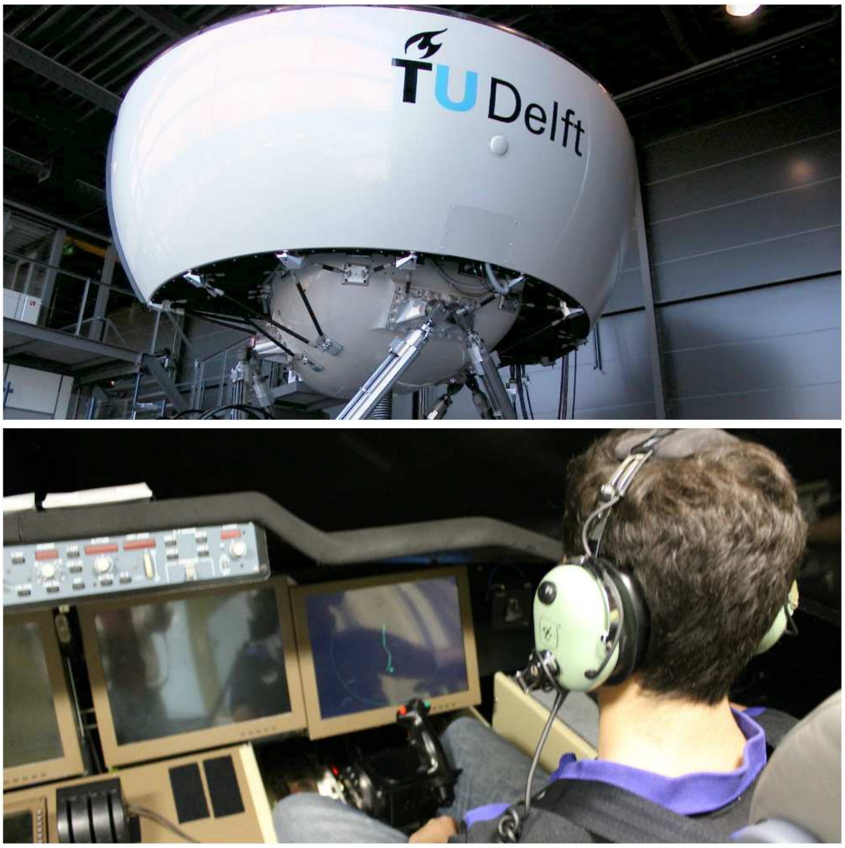

TU Delft Delft University of Technology

Challenge the future

The Role of Motion Feedback in Manual Preview Tracking Tasks

Master of Science Thesis

For obtaining the degree of Master of Science in Aerospace Engineering
at Delft University of Technology

J. Morais Almeida

August 24, 2016

Faculty of Aerospace Engineering · Delft University of Technology

Delft University of Technology

Delft University Of Technology
Department Of
Control and Simulation

The undersigned hereby certify that they have read and recommend to the Faculty of Aerospace Engineering for acceptance a thesis entitled **"The Role of Motion Feedback in Manual Preview Tracking Tasks"** by **J. Morais Almeida** in partial fulfillment of the requirements for the degree of **Master of Science**.

Dated: August 24, 2016

Readers:

prof.dr.ir. M. Mulder

dr.ir. M. M. van Paassen

dr.ir. D. M. Pool

ir. K. van der El

dr.ir. W. Mugge

Acknowledgments

Over the past seven months of work, a lot of people helped me in this investigation and in writing this master thesis. Some of them helped directly, by lending their expertise and knowledge, while others were just as important with their support throughout these months.

I would like to thank my daily supervisors, Daan and Kasper, for all the time, patience and effort they put into this project. It was a pleasure to work with both of you, and the challenges and comments you made about my work made me strive to be the best I could. I learned a lot from both of you in these seven months. I would also like to thank Max and Rene, for making time when it was needed for my project and for their interest on it.

For all the time spent in the simulator, getting me the data I needed for the experiment, I need to thank David, Dirk, Filipe, Isaac, Ivan, Laurens, Martijn, Matej, Rick, Tao, Wei. Thank you for taking the time to be inside a simulator for a few hours.

I also need to thank all the people that worked alongside me almost every day, for always being there to ask or answer every small question and daily frustration: Diogo, Joao Paulo, Joao, Miguel, Pedro, Ricardo and Tomas.

Last but not the least, I need to thank all the people back home, who may not have been physically present, but were indeed present through this project. First, my family, for giving me the wonderful opportunity of studying here, and for being present to hear all my complaints and cheer my victories. Second, all the friends who helped me be at my best every day, and whom I thank from the bottom of my heart, a list too long to be written here. Thanks to all of you I felt close to home, even being this far away. You certainly know who you are, and this project is also a bit from each and every one of you. Thank you.

Acronyms

ANOVA	Analysis of Variance
CS	Control and Simulation
DUT	Delft University of Technology
FC	Fourier Coefficients
NMS	Neuromuscular System
NVP	Near-Viewpoint Response
SRS	SIMONA Research Simulator
TX	Target-Feedthrough and State-Feedback
VAF	Variance Accounted For

List of Symbols

Greek Symbols

Γ	coherence
ω	radial frequency
ϕ	phase angle
σ	standard deviation
τ	time shift
Θ	parameter vector
ζ	damping ratio

Roman Symbols

A	amplitude
E	Fourier transform of the error
e	error
F	Fourier transform of the forcing function
f	forcing function
H	frequency response function
j	imaginary unit
K	gain
N	Fourier transform of the remnant
n	remnant
P	periodogram
S	power spectral density function

T	time constant
t	time
U	Fourier transform of the control input
u	control input
X	Fourier transform of the output
x	output

Subscripts

b	base
c	crossover
ce	controlled element
d	disturbance
e	error
$e^{\star}$	internal-error response
f	far-viewpoint
i	input
L	lead
l	lag
m	motion
n	near-viewpoint
nms	neuromuscular system
ol	open-loop
p	preview
scc	semi-circular canals
t	target
u	control output
v	visual
x	system output

Contents

List of Figures

List of Tables

Report Overview

This is the report of the final graduation thesis of J. Morais Almeida on "The Role of Motion Feedback in Manual Preview Tracking Tasks". It is divided in two parts.

The first part includes the graduation paper, which details a human-in-the loop experiment performed in order to validate the use of a model for preview including motion feedback.

The second part contains the book of appendices, which includes all the details of the experiment that were not presented in the paper. This includes the experiment briefing, the Latin-Square experiment design, the choice of control variables and individual subject results for variance, coherence, describing functions and model parameters. It also contains the comparison of the model with and without near-viewpoint, and the comparison between two different models for preview with motion feedback.

Part I

Paper - The Role of Motion Feedback in Manual Preview Tracking Tasks

The Role of Motion Feedback in Manual Preview Tracking Tasks

João Morais Almeida, Kasper van der El, *Student Member, IEEE,* Daan M. Pool, *Member, IEEE,* Marinus M. van Paassen, *Senior Member, IEEE* and Max Mulder

***Abstract*—Motion feedback has an important effect in many tasks performed by humans. In this paper, we aim to investigate the role of motion feedback in preview tracking tasks with double integrator dynamics, using results from a human-in-the-loop experiment performed in the SIMONA Research Simulator of the Delft University of Technology. Eight subjects performed the same yaw tracking task with a compensatory and preview display, both with and without motion feedback. System identification techniques and quasi-linear human controller models for preview and motion feedback are used to explain human controller's behavior in tracking tasks. An extension to an existing human preview control model is proposed, in order to model the human in a preview task using motion feedback. It is found that, when motion feedback is available, human controllers adapt their behavior in a similar way for compensatory and preview tasks. Motion feedback allows human controllers to further improve their performance in preview tracking. This research shows for the first time that motion feedback still has an important effect on the human controller behavior, even if visual preview is available.**

I. Introduction

THE topic of manual control has been widely studied in the scientific community. McRuer and his colleagues [9] developed the widely known "crossover model", which models how humans perform a task using a compensatory display. This enables obtaining a mathematical model for humans in a very simple task, where only the error is displayed. Obtaining such a model for more realistic tasks, where more information is present (more visual feedbacks, motion feedback) would allow for a more complete understanding of manual control.

Research has previously been conducted on the role of motion feedback in compensatory tasks ([3], [4], [7], [13], [14], [15], [18], [27]). Not only was motion feedback found to result in improved tracking performance, but also extensions to the crossover model including motion feedback were proposed. The main drawback of the compensatory task is that it translates poorly to real-life tasks. The preview task, in which the future movement of the target is also shown to the human, is closer to what can be seen in the real world, in tasks such as driving a vehicle along a road. A number of preview models have been proposed throughout the years, based on optimal control ([5], [19], [21]) or driving models ([2], [8], [17]), among others. Recent research at the Delft University of Technology proposed a new empirical model for this kind of task ([22], [23]). This model allows to understand how humans use preview, by using both feedforward and feedback control.

The authors are with the Control and Simulation section, Faculty of Aerospace Engineering, Delft University of Technology, 2629 HS Delft, The Netherlands.

It is still not clear if human controllers use preview similarly in tasks using motion feedback, and if motion feedback is still beneficial in preview tracking tasks. This paper investigates the role of motion feedback in preview tracking tasks, by analyzing how both feedbacks affect performance, and human tracking behavior.

An experiment was conducted in the SIMONA Research Simulator at the Delft University of Technology. Subjects performed a yaw tracking task using a double integrator controlled element, with compensatory and preview displays, both with and without motion feedback. An offline model simulation was performed in order to predict what the effect of the motion feedback would be in preview tracking tasks. Coherence was calculated as a measure of linearity of the human controller. Error and control output variances were obtained, and system identification methods were used to identify the pilot response. The van der El model [22] was then fitted to the experimental data, with an extension for the case of preview with motion feedback. The Variance Accounted For is calculated as a measure of the quality of the model fit.

This paper is structured in seven sections. In Section II, the control task is presented, along with the models used for compensatory tasks, with and without motion, and preview tasks. An extended model is proposed for the preview tracking task with motion, which is used in Section III, to perform offline model simulations. The description of the human-in-the-loop experiment and the system identification techniques used are presented in Section IV. Section V contains the experiment results, and Section VI the discussion of these results. This paper ends with the conclusions in Section VII.

II. Control Task

A. Task Characteristics

The control task considered in this paper is a combined target-tracking and disturbance-rejection task. In a target-tracking task, the human controller is asked to track a target signal, designated by $f_t(t)$, minimizing the error $e(t)$ between the output $x(t)$ and the current target [9]. This output can also be perturbed by a disturbance signal $f_d(t)$, which constitutes the disturbance-rejection part of the task.

In this paper, control tasks performed with compensatory and preview displays are investigated. In the compensatory task, only the error is displayed. In the preview task, the human controller can see the future target signal up to τ_p seconds ahead. These displays can be seen in Figure 1. Both displays were chosen to have an "inside-out" representation, with a static output marker (a circle) and a moving target. In the compensatory case (Figure 1 (a)), the target is represented by a cross. In the preview case (Figure 1 (b)) the current target is the bottom ($\tau_p = 0$) of the preview line.

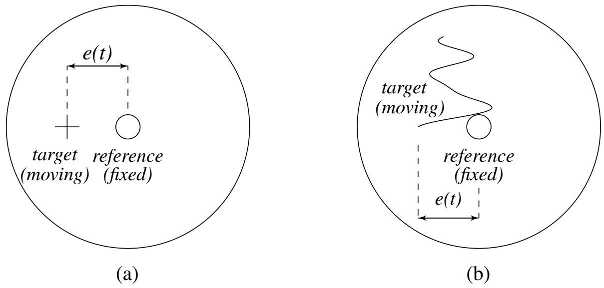

Fig. 1: The compensatory (a) and preview display (b)

The controlled element used in these tracking tasks can take a different number of forms, including models that approach aircraft dynamics to simpler systems such as gain, single integrator and double integrator. In this paper, the focus will be on the double integrator controlled element, since it is the case in which the motion feedback is found to have a larger effect on performance and the highest motion use, according to [7]. The controlled element used in this control task was given by:

$$H_{ce}(j\omega) = \frac{5}{(j\omega)^2} \tag{1}$$

B. Human Controller Modeling in Compensatory Tasks

In the following sections, the human controller modeling approaches in literature will be presented. These approaches follow the control diagram of Figure 2. This diagram presents the McRuer *et al.* in [9] model extended with an additional motion feedback channel (shown in a dashed rectangle) proposed by Hosman [3].

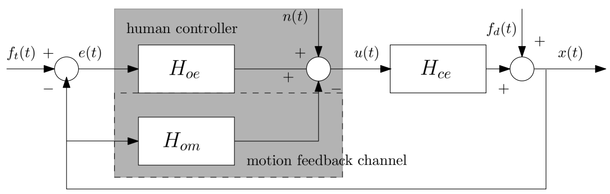

Fig. 2: Compensatory model with motion feedback channel

1) Compensatory Tracking: A compensatory tracking task is defined as a task in which only the current error, $e(t)$, is presented to the human controller. For this type of task, an empirical model has been derived by McRuer *et al.* in [9]. McRuer proposed a quasi-linear model to explain the behavior of the human controller in such a task, in which the operator is described by a linear frequency response function $H_{oe}(j\omega)$, and a non-linear part $n(t)$, the remnant signal.

The proposed model states that humans adapt their control dynamics so that, in the crossover region (around a crossover frequency ω_c), the open-loop describing function approximates a single integrator with a time delay, as in Equation (2) [9].

$$H_{ol}(j\omega) = H_{o_e}(j\omega)H_{ce}(j\omega) = \frac{\omega_c}{j\omega}e^{-j\omega\tau_v} \tag{2}$$

The operator frequency response function $H_{oe}(j\omega)$ is modeled for a double integrator as in Equation (3).

$$H_{oe}(j\omega) = K_e(1 + T_{L,e}j\omega)e^{-\tau_v j\omega}H_{nms}(j\omega) \tag{3}$$

In this model, K_e represents the human controller response gain, $T_{L,e}$ the lead time constant, τ_v the visual time delay and H_{nms} the neuromuscular dynamics. The neuromuscular dynamics are typically modeled ([7], [15]), as seen in Equation (4), with ω_{nms} the natural frequency of the neuromuscular system and ζ_{nms} the damping ratio.

$$H_{nms}(j\omega) = \frac{\omega_{nms}^2}{(j\omega)^2 + 2\zeta_{nms}\omega_{nms}j\omega + \omega_{nms}^2} \tag{4}$$

2) Role of Motion Feedback: The effect of motion feedback in compensatory tracking tasks is well documented in literature ([3], [4], [7], [13], [14], [15], [18], [27]). Hosman and Van der Vaart [4] found that motion cues significantly improved performance. For the target-following task, a reduction in the target crossover frequency ω_{ct} and an increase in the target phase margin ϕ_{mt} are found. Regarding disturbance rejection, the study found an increase in the disturbance phase margin ϕ_{md} and in the disturbance crossover frequency ω_{cd}. Schroeder [18] and Pool *et. al* [15] later confirmed these findings. In [13], a compilation of a large number of research studies on the field was obtained, and these findings were found to be a general trend, apart from the phase margins. For both the target and disturbance phase margins, motion was found not to have an effect in this research. According to Hosman [3], the motion feedback is modeled as an extra feedback path, with a frequency response function including the semi-circular canal dynamics:

$$H_{o_m}(j\omega) = (j\omega)^2 H_{scc}(j\omega)K_m e^{-\tau_m j\omega} \tag{5}$$

The most remarkable effect of motion feedback in compensatory tasks is an increase in performance. With motion feedback, human controllers adapt their control strategy, by increasing the error response gain K_e. The lead generated by the motion feedback channel allows human controllers to generate less visual lead, which is shown by the decrease in the lead time constant $T_{L,e}$. The task then becomes easier for the human controller, which is shown by an increase in the disturbance crossover frequency [15], [13], [7].

C. Human Controller Modeling in Preview Tasks

In this paper, a new model for preview tracking tasks is proposed which combines the previous research on compensatory tasks with the van der El *et. al* model [22] for preview tasks without motion feedback. The extension adds an extra feedback path to the preview model, as can be seen in Figure 3. This control diagram shows the hypothesized additional motion channel with a dashed line.

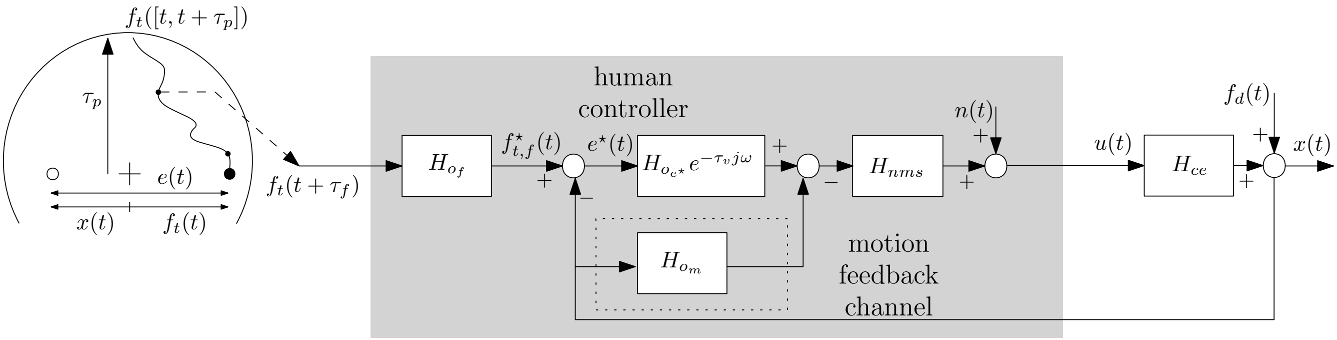

Fig. 3: Preview model proposed by Van der El *et. al* ([22]) including a motion channel

1) Preview Tracking: Van der El *et. al* proposed a model for preview tracking in which the response of the human controller to a previewed target trajectory is captured by a response to two different points ahead: the near-viewpoint $f_{t,n}$ and the far-viewpoint $f_{t,f}$:

$$f_{t,n} = f_t(t + \tau_n) \qquad f_{t,f} = f_t(t + \tau_f) \tag{6}$$

No near-viewpoint was included in the proposed model, since in previous studies it is found to be difficult to determine whether it is actually being used by the human controller [23] and its contribution to the human controller's output is generally small for a double integrator controlled element. This allows to reduce the number of parameters to estimate, yielding lower estimation uncertainties in the remaining parameters, as used in [11].

The far-viewpoint response is modeled as a low-pass filter, as the human controller uses it to track the low frequencies of the target signal:

$$H_{o_f}(j\omega) = K_f \frac{1}{1 + T_{l,f} j\omega}, \tag{7}$$

in which K_f is the far-viewpoint gain and $T_{l,f}$ is the far-viewpoint lag time constant.

The human controller responds to an error $e^{\star}$, defined as the difference between the target filtered by the far-viewpoint dynamics and the controlled element output:

$$E^{\star}(j\omega) = F^{\star}_{t,f}(j\omega) - X(j\omega) = H_{o_f} F_t(j\omega) - X(j\omega) \tag{8}$$

The dynamics of the internal-error response resemble the equalization term of compensatory tracking, as can be seen in Equation (9) for a double integrator controlled element.

$$H_{o_{e^\star}}(j\omega) = K_{e^\star}(1 + T_{L,e^\star} j\omega) \tag{9}$$

in which $K_{e^\star}$ is the error response gain, $T_{L,e^\star}$ is the lead time constant.

The human controller can respond to the output, the target and the error, in a total of three describing functions. Using two external signals, the target and the disturbance, only two operator describing functions can be identified. The model is then typically restructured to a a two-channel model, with H_{o_t} representing the response to the target and H_{o_x} the response to the controlled element output [22], [23], [11], see Figure 4. These lumped dynamics are defined as:

$$\begin{aligned} H_{o_t}(j\omega) = & [H_{o_f}(j\omega) H_{o_{e^\star}}(j\omega) e^{\tau_f j\omega} \\ & + H_{o_n}(j\omega) e^{\tau_n j\omega}] H_{nms}(j\omega) e^{-\tau_v j\omega} \end{aligned} \tag{10}$$

$$H_{o_x}(j\omega) = H_{o_{e^\star}}(j\omega) H_{nms}(j\omega) e^{-\tau_v j\omega} \tag{11}$$

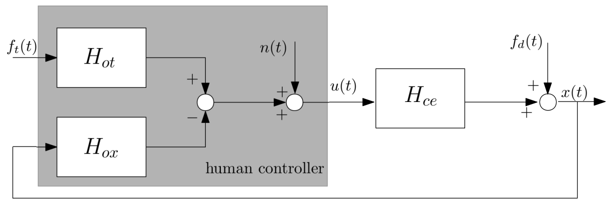

Fig. 4: Model with lumped dynamics in TX (target and output response) form, as in Van der El *et. al* ([22] - [23])

2) Proposed model for Preview with Motion Feedback: The proposed model for preview tracking accounting for motion feedback can be converted to the same lumped structure of Figure 4 by adding the H_{o_m} frequency response function to Equation (11), while there is no change in Equation (10).

$$H_{o_x}(j\omega) = H_{o_{e^\star}}(j\omega) H_{nms}(j\omega) e^{-\tau_v j\omega} + H_{o_m}(j\omega) H_{nms}(j\omega) \tag{12}$$

In this equation, H_{o_m} uses the same structure as Equation (5). The normalized semi-circular canals model was used, as in [16]. This model includes a gain which ensures the model has an unitary absolute value at 1 rad/s.

$$H_{scc}(j\omega) = \frac{5.97(0.11 j\omega + 1)}{(5.9 j\omega + 1)(0.005 j\omega + 1)} \tag{13}$$

It should be noted that the proposed model doesn't introduce a large change in the existing preview model: in fact, the H_{o_m} equation can be simplified over a range of frequencies to:

$$H_{o_m}(j\omega) = |(j\omega)| K_m e^{-\tau_m j\omega} \tag{14}$$

On the other hand, for a double integrator, $H_{o_{e^\star}}$ including the visual time delay is given by:

$$H_{o_{e^\star}} = K_{e^\star} e^{-\tau_v j\omega} + K_{e^\star} T_{L,e^\star} j\omega e^{-\tau_v j\omega} \tag{15}$$

It can be seen that the second term of Equation (15) has the same structure of the additional H_{o_m} path in the proposed model. It can then be expected there is undesired redundancy in the proposed model, which may lead to problems in the identification of its parameters.

III. Offline Model Simulations

Offline human control model simulations were performed using the proposed model (Figure 3) to predict the possible the benefit of motion feedback and using an H_{om} response in preview tracking tasks. The findings are presented in this section.

A. Simulation settings

In order to predict the human controller's adaptation to motion feedback, the response of the proposed model is simulated for increasing values of the motion gain K_m, while all other model parameters (eg. H_{oe}, H_{of}) are kept constant. This simulation was performed both for compensatory and preview tasks.

The proposed model includes two motion parameters: the gain K_m and the and the motion delay τ_m. Since the motion time delay τ_m is consistently found around 0.2 in literature [7], it was fixed at that value. The gain K_m was changed from 0 (no motion) to 0.25 in increments of 0.05. This maximum gain was defined as further increase in the motion gain causes instability for the preview condition.

B. Model settings

The settings used for the offline model simulations can be seen in Table I. The controlled element was a double integrator given by $5/(j\omega)^2$. The compensatory parameters were based on the results of [7] and the preview model parameters were taken from the results of [22].

TABLE I: Parameters for offline model simulations

Conditions	$K_{e^\star}, -$	$T_{L,e^\star}, s$	$\omega_{nms}, rad/s$	$\zeta_{nms}, -$
Compensatory	0.20	1.70	12	0.40
Preview	0.20	2	6	0.45
	τ_v, s	$K_f, -$	$T_{l,f}, s$	τ_f, s
Compensatory	0.30	1	0	0
Preview	0.30	0.9	1	1

C. Results

The error and control output variances were calculated to quantify performance and control output, respectively. Open-loop describing functions were also used to calculate the crossover frequency and phase margin for each value of K_m.

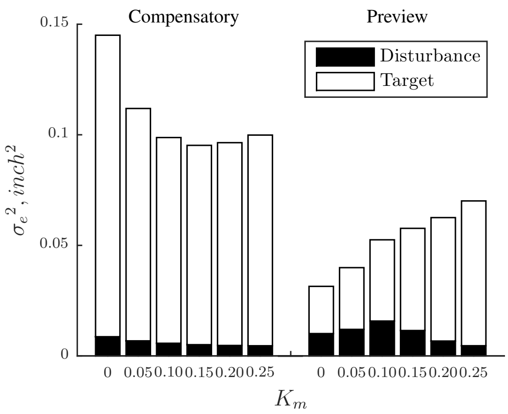

(a)

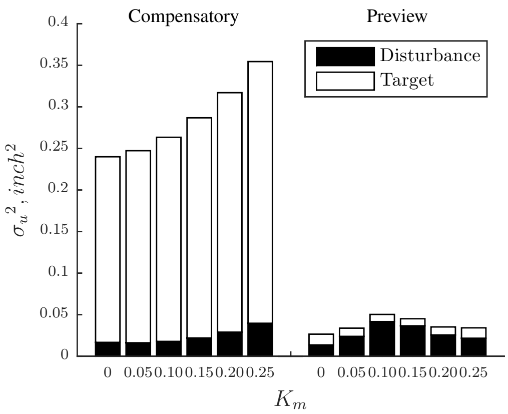

(b)

Fig. 5: Variance of the error (a) and control output (b) for increasing magnitude of the motion feedback channel

1) Tracking Performance and Control Activity: In Figure 5 the variance of the error and control output are displayed.

When no motion feedback is available, there is a clear increase in performance when preview is used, with a total decrease in the variance of the error of 64%. It should be noted that this increase in performance is largely due to the target frequencies, in which there is an 84% decrease in the variance of the error.

Regarding the motion feedback in the compensatory case, a performance improvement is found as K_m increases. Even without any adaptation in the other parameters, the use of motion feedback improves performance in compensatory tracking, as found in previous experiments [4], [18], [15], [27], [13], [7].

For the preview case, there is an increase in the error when motion feedback is used. However, it can be seen that there is a better tracking of the disturbance frequencies, with the increase in error caused by the target frequencies.

2) Crossover Frequency and Phase Margin: In Figures 6 and 7, the crossover frequency and phase margin of the offline model simulations are displayed.

For the crossover frequency, the same trend is found for the

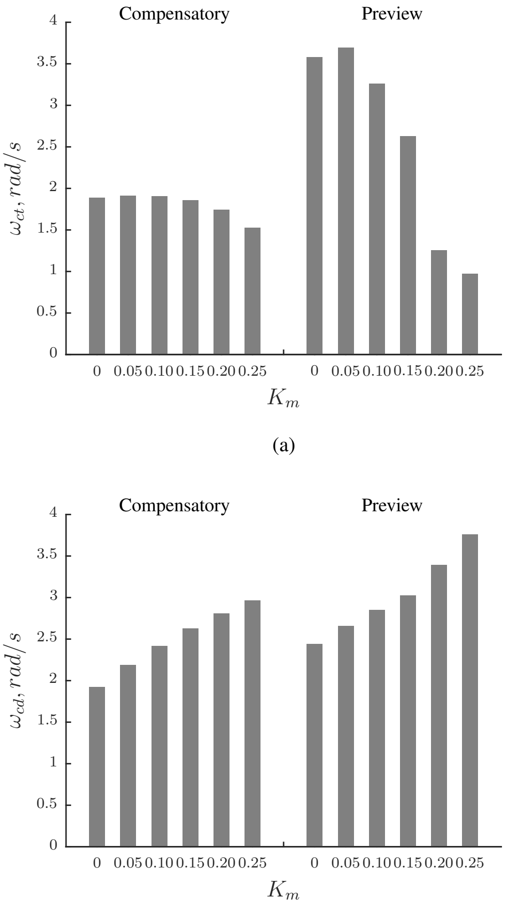

(a)

(b)

Fig. 6: Target (a) and disturbance (b) crossover frequency for increasing magnitude of the motion feedback channel

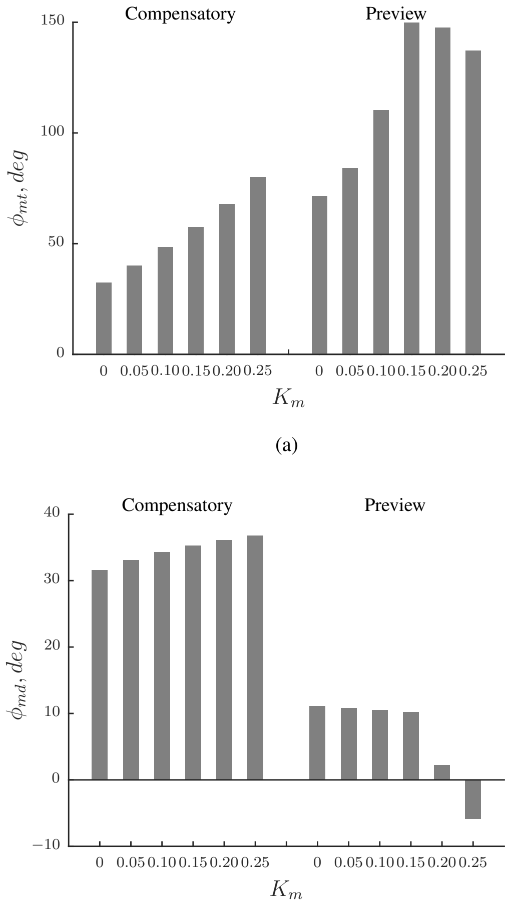

(a)

(b)

Fig. 7: Target (a) and disturbance (b) phase margin for increasing magnitude of the motion feedback channel

compensatory and preview simulations. The target crossover frequency ω_{ct} decreases when motion is added, and the disturbance crossover frequency ω_{cd} increases. These results are in line with previous results in literature [4], [18], [15], [13], [7].

Regarding the phase margin, it can be seen that the target phase margin ϕ_{mt} increases when motion is added, mostly on the preview case. On the disturbance phase margin ϕ_{md}, however, the compensatory and preview tasks show a substantial difference: while there is only a modest increase in the compensatory case (as seen in [4], [18], [15], [7]), for the preview case it decreases and eventually becomes negative, indicating the closed-loop becomes unstable.

IV. Method

A. Hypotheses

Regarding the effect of motion feedback, and the previous research summarized in Section II-B, it is known that motion has a marked effect on tracking performance and human control behavior in tracking tasks with double integrator dynamics. It is thus hypothesized that:

I When motion feedback is added, there will be an increase in performance for compensatory tasks and human controller adaptation. The human adaptation will be clear by an increase in the error response gain K_e, a decrease in the lead time constant T_{L_e} and a non-zero gain K_m.

When a human controller is provided with preview, he has the ability to look ahead and respond not only to the error, but also to the future target, which allows for better performance [23]. Therefore, in accordance with the findings in [23], the following hypothesis is drawn:

II Availability of preview information allows human controllers to improve their target-tracking performance. by responding to . The use of preview introduces a negative time delay τ_f in the system, which allows the human controller to respond to an internal-error $e^{\star}$, filtered by the far-viewpoint response H_{of}.

On the one hand, the offline model simulations predicted a degradation in performance when motion feedback is included in the preview task. The disturbance-rejection, however, is improved in the simulations. On the other hand, compensatory tracking literature finds a significant improvement in performance when motion feedback is added. It is also known that human controllers adapt their behavior when motion feedback is available, which was not considered in the offline model simulations, and may influence target-tracking behavior. It is then hypothesized that:

III For preview tracking, the tracking performance will be improved on the disturbance frequencies when motion feedback is available. Using motion feedback, the human controller is able to close an additional motion channel H_{om}, and it is expected that the human controller adaptation will be similar to what was compensatory tracking tasks, with an increase in the error response gain K_e and a decrease in the lead time constant T_{L_e}.

B. Independent Variables

The experiment considered two independent variables: the display type and the presence of motion feedback. The displays had either compensatory or preview configuration, see Figure 1. The motion feedback was either off or on. A full-factorial design was used, so all combinations of the independent variables were tested by each participant. This yields a total of four conditions, as it can be seen in Table II.

TABLE II: EXPERIMENTAL CONDITIONS DEFINITION

	Motion on	*Motion off*
Compensatory	C	CM
Preview	P	PM

C. Apparatus

The experiment was conducted in the SIMONA Research Simulator (SRS) at the Delft University of Technology (see Figure 8). The subjects were seated in the right seat of the simulator, using an electric sidestick to give an input to the system. The stick was fixed in the pitch axis and could only rotate around its roll axis.

Fig. 8: The SIMONA Research Simulator

The displays were presented on the primary flight display of the simulator, directly in front of the subjects, with green lines and indicators on a black background. These displays were either compensatory or preview, as can be seen in Figure 1.

D. Control Variables

Two seconds of preview are displayed on the screen, well above the critical preview time found in [11]. The critical preview time is defined as the length of preview above which there is no improvement in the tracking performance.

The motion cue used in the experiment was the yaw rotation of the simulator, and was the same for all the conditions including motion feedback. The yaw rotation was corrected so that the motion axis was centered in the right seat of the simulator and not on the centroid of the simulator. Motion was presented one to one, without no washout.

E. Forcing Functions

To facilitate the use of system identification methods described in Section IV-H, the forcing functions in the experiment were defined as a sum of sinusoids given by Equation (16). The same expression was used for the disturbance and target forcing functions.

$$f_{t,d}(t) = \sum_{k=1}^{20} A_{t,d}[i] \sin(\omega_{t,d}[i]t + \phi_{t,d}[i]) \tag{16}$$

In this expression, f stands for the forcing function signal, and A, ω and ϕ for the sinusoid amplitude, frequency and phase, respectively.

Both target and disturbance amplitudes were defined using a second-order low-pass filter, as used in [15] and [27]. The absolute value of the filter at a given frequency yields the sinusoid amplitude. This filter is defined in Equation (17).

$$H_A(j\omega) = \frac{(1 + 0.1j\omega)^2}{(1 + 0.8j\omega)^2} \tag{17}$$

This amplitude distribution results in a realistic and not too difficult task for the subjects [27]. This is also the same amplitude distribution used in previous yaw motion experiments, such as [7]. In order to avoid leakage and allow the use of spectral analysis, the frequencies used were integer multiples of the base frequency ω_b. Each run consisted of a measurement time of 120 seconds, which yields a base frequency $\omega_b = 2\pi/120 = 0.0524$ rad/s. To allow for the calculation of coherence, double bands of frequencies were used [22]. The frequencies used were the same as in [22] and [23], in a total of 20 sinusoids.

Five different target signals were used, different only on the phases ϕ_t, to avoid memorization of the signal by the subjects. For the disturbance signal only one realization was used, as it is unlikely the subjects would memorize it since it is not directly displayed. Given that in the SRS the disturbance is inserted before the controlled element, it was pre-filtered with the inverse dynamics of the controlled element. The standard deviation of the target forcing function was 4.5 degrees and of the disturbance forcing function was 1.8 degrees. The spectra of the forcing function signals are shown in Figure 9. The parameters of the forcing functions are given in Table III.

TABLE III: PARAMETERS OF THE TARGET AND DISTURBANCE FORCING FUNCTION SIGNALS

	target signals f_t								disturbance signal f_d			
k, -	n_t, -	A_t, deg	ω_t, rad/s	$\phi_{t,1}$, rad	$\phi_{t,2}$, rad	$\phi_{t,3}$, rad	$\phi_{t,4}$, rad	$\phi_{t,5}$, rad	n_d, -	A_d, deg	ω_d, rad/s	ϕ_d, rad
1	2	0.308	0.105	0.028	1.156	1.278	4.752	5.105	5	0.002	0.262	4.755
2	3	0.305	0.157	2.299	1.783	2.651	5.326	5.492	6	0.003	0.314	4.937
3	8	0.279	0.419	5.953	3.655	2.051	6.104	2.667	11	0.008	0.576	2.393
4	9	0.272	0.471	3.439	3.364	0.485	2.841	2.400	12	0.009	0.628	3.470
5	14	0.232	0.733	1.048	3.212	4.286	0.963	4.079	18	0.016	0.942	5.278
6	15	0.223	0.785	1.400	5.901	1.352	4.758	3.739	19	0.017	0.995	4.326
7	26	0.144	1.361	1.621	3.074	1.594	0.771	1.172	31	0.028	1.623	4.749
8	27	0.139	1.414	1.898	1.524	4.749	4.072	6.025	32	0.028	1.676	0.955
9	40	0.085	2.094	2.102	2.243	3.535	1.349	1.687	58	0.040	3.037	1.814
10	41	0.082	2.147	5.420	0.597	0.077	1.743	4.791	59	0.040	3.089	4.670
11	78	0.031	4.084	3.360	5.938	0.100	3.871	4.744	93	0.050	4.869	3.346
12	79	0.030	4.136	5.704	4.734	5.516	6.049	1.418	94	0.050	4.922	0.692
13	110	0.019	5.760	5.208	1.430	5.653	3.549	2.992	128	0.060	6.702	2.158
14	111	0.018	5.812	0.444	4.074	5.578	4.000	3.609	129	0.060	6.754	2.564
15	148	0.013	7.749	1.701	2.713	5.727	0.166	3.945	158	0.070	8.273	3.903
16	149	0.012	7.802	5.457	1.973	5.008	4.221	1.730	159	0.071	8.325	3.219
17	177	0.010	9.268	5.847	4.698	5.807	0.152	3.959	193	0.085	10.105	1.609
18	178	0.010	9.320	1.693	1.381	1.580	4.410	3.193	194	0.086	10.158	4.606
19	220	0.008	11.519	6.016	4.907	4.945	2.747	3.365	301	0.148	15.760	0.889
20	221	0.008	11.572	0.713	3.805	3.827	1.411	2.490	302	0.149	15.813	5.525

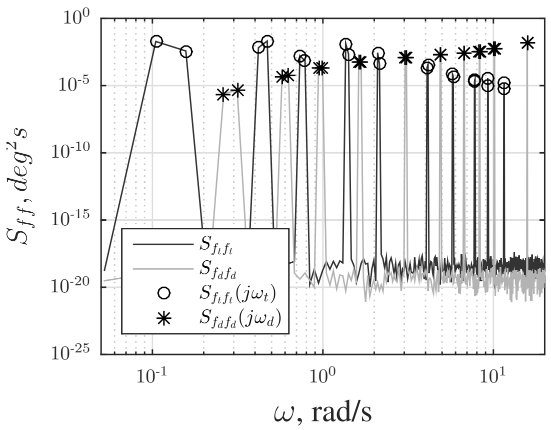

Fig. 9: Single-sided Power Spectral Density of the forcing function signals

F. Experimental Procedure

The experiment was performed by eight male volunteers aged between 22 and 32 years old. Their experience in tracking tasks ranged from little practice to extensive experience. All the subjects were briefed before participating, and given all necessary instructions to perform the experiment.

For each subject, a task familiarization was performed before the actual experiment, in which each condition was tried at least once. After this phase, the measurement phase begun. The order of the conditions was randomized using a balanced Latin-Square distribution among the subjects. For each condition, each subject performed three training runs, and an extra five to twelve runs, until stable performance was achieved. Only the last five runs of each condition for each subject were used for data analysis.

After every run, the experimenter reported the score to the subjects, using the root-means-square of the error. Each run lasted for 132 seconds, of which the first eight seconds were run-in time and the last four were fade-out time, with 120 seconds being used as measurement time. Breaks were taken between every two conditions. The total experiment time, breaks included, was around three hours per subject.

G. Dependent Variables

In this experiment, the variances of the error and control output are used quantify performance and control activity. Coherence is calculated to validate the use of a quasi-linear model for the human controller. Open-loop describing functions are calculated in order to obtain crossover frequencies and phase margins to quantify performance in the frequency domain and closed-loop stability. Black-box identification and parameter estimation are used to obtain the frequency response of the human controller. Model parameters are obtained based on the proposed model in order to understand the human behavior in the control task. Model VAFs are obtained in order to quantify the ability of the model to describe the output.

H. Data Analysis

1) Coherence: The coherence is a measure for the linear relationship between two signals. It can range from 0 to 1, where 0 means no linear relation and 1 means completely linear relation. The coherence is calculated to verify the linearity of the human controller's inputs in response to the applied forcing functions. A high coherence shows that the relation is close to linear, which means that quasi-linear models can be applied to model the human controller dynamics REF. Equation (18) shows how coherence is estimated for the target signal. Calculation for the disturbance signal is analogous.

$$\Gamma_{f_t,u}(\tilde{\omega}_t) = \sqrt{\frac{|\tilde{P}_{f_t u}(\tilde{\omega_t})|^2}{\tilde{P}_{f_t f_t}(\tilde{\omega}_t)\tilde{P}_{uu}(\tilde{\omega}_t)}}, \tag{18}$$

In this equation, $\tilde{\omega}$ is the average frequency between two frequencies in a double band, and $\tilde{P}$ is the average periodogram of the respective subscripted signals at that average frequency.

2) Open-loop Describing Functions: Open-loop describing functions allow to further understand the performance and the stability of the system. The measures used are the crossover frequency ω_c, which corresponds to the frequency at which $|H_{ol}(j\omega)| = 1$, and the phase margin ϕ_m defined by $180 + \angle H_{ol}(j\omega_c)$. The open-loop describing functions are defined, for a combined target-tracking and disturbance-rejection tracking tasks, as in [6]:

$$\begin{aligned} H_{ol,t}(j\omega_t) =& \frac{X(j\omega_t)}{E(j\omega_t)} \\ =& \frac{H_{o_t}(j\omega_t)H_{ce}(j\omega_t)}{1 + [H_{o_x}(j\omega_t) - H_{o_t}(j\omega_t)]H_{ce}(j\omega_t)} \end{aligned} \tag{19}$$

$$\begin{aligned} H_{ol,d}(j\omega_t) =& \frac{X(j\omega_d) - F_d(j\omega_d)}{X(j\omega_d)} \\ =& H_{ce}(j\omega_d)H_{o_x}(j\omega_d) \end{aligned} \tag{20}$$

3) Black-Box Multiloop System Identification: For system identification, a black-box, Fourier coefficient based method is used, as described in [24]. For the introduced two-channel model (see Figure 4), Equation (21) can be obtained, in which U, F_t and X are the Fourier transforms of the control output, the target forcing function and the controlled element output, respectively. This equation excludes the remnant, as it is considered small at the input frequencies [24].

$$U(j\omega) = H_{o_t}(j\omega)F_t(j\omega) - H_{o_x}(j\omega)X(j\omega) \tag{21}$$

This equation contains two different describing functions, H_{o_t} and H_{o_x}. In order to solve for both describing functions, a second equation is required. This equation can be obtained by evaluating Equation (21) only at the signal input frequencies, while also interpolating the Fourier transforms at the disturbance frequencies to the target frequencies, yielding the signals $\tilde{U}$, $\tilde{F}_t$ and $\tilde{X}$. This yields a system of two equations and two unknowns, given by Equation (22), which can be solved for H_{o_t} and H_{o_x}. The same process is performed for the disturbance frequencies, so that H_{ot} and H_{ox} estimates are obtained at all excited frequencies.

$$\begin{bmatrix} U(j\omega_t) \\ \tilde{U}(j\omega_t) \end{bmatrix} = \begin{bmatrix} F_t(j\omega_t) & -X(j\omega_t) \\ \tilde{F}_t(j\omega_t) & -\tilde{X}(j\omega_t) \end{bmatrix} \begin{bmatrix} H_{o_t}(j\omega_t) \\ H_{o_x}(j\omega_t) \end{bmatrix} \tag{22}$$

4) Parameter Estimation: The model parameters were obtained by minimization of a cost function J, given in Equation (23).

$$J(\Theta) = \sum_{i=1}^{N_t} |U(j\omega_i) - \hat{U}(j\omega_i|\Theta)|^2 \tag{23}$$

with

$$\hat{U}(j\omega_i|\Theta) = \hat{H}_{o_t}(j\omega_i|\Theta)F_t(j\omega_i) - \hat{H}_{o_x}(j\omega_i|\Theta)X(j\omega_i) \tag{24}$$

This cost function is the difference between the measured and modeled control output, at a number N_t of ω_i frequencies below a cut-off frequency, chosen at 25 rad/s. The parameter vector Θ is defined as $[K_{e^\star}\ T_{L,e^\star}\ \tau_v\ \omega_{nms}\ \zeta_{nms}\ K_f\ T_{l,f}\ \tau_f,\ K_m,\ \tau_m]^{\mathrm{T}}$.

In order to minimize J, a Nelder-Mead algorithm was used, with the MATLAB function *fminsearch()*. It was constrained to discard only negative parameters. 10,000 initial parameter sets are randomly generated and the 100 with the lowest cost function are used as starting points for the optimization. The solution with the lowest cost is considered the best solution.

5) Variance Accounted For: The Variance Accounted For (VAF) is used as a measure of the similarity of two signals. A maximum value of 100% means that the signals are identical. It can then be used to compare the modeled and measured control output, to quantify how well the model represents the human controller behavior. The VAF is given by:

$$VAF = \left(1 - \frac{\sum_{k=1}^{N_s} P_{\epsilon_u \epsilon_u}(k\omega_b)}{\sum_{k=1}^{N_s} P_{uu}(k\omega_b)}\right) \times 100\%, \tag{25}$$

with ϵ_u the modeling error ($U(j\omega_k) - \hat{U}(j\omega_k|\Theta)$) and N_s is the total number of samples.

6) Data Processing: Coherence was calculated per subject and per run. The results were averaged over five runs and then averaged over the eight subjects, for each condition. The variances of the error and control output were calculated for individual runs and averaged for each subject. These variances were calculated by integration of power spectral densities, in order to allow separation of the contributions of target, disturbance and remnant frequencies [6]. The frequency response functions were estimated using the frequency-domain average of the five measurement runs for each subject, in order to reduce noise. The phase margins and crossover frequencies were calculated using the estimated frequency response functions, using Equation (19) and (20). The Variance Accounted For is calculated per subject, based on the obtained models.

A two-way repeated measures ANOVA was applied to test for significant changes in tracking performance, control activity, crossover frequency and phase margin. 95% confidence intervals of the variances, crossover frequencies, phase margins and model parameters were corrected for between-subject variability.

V. Results

A. Tracking Performance and Control Activity

Figure 10 shows the average variances of the tracking error e and the control output u, for each condition. Each bar also shows the contributions of the target, disturbance and remnant frequencies. The 95% confidence intervals of the means of the total σ_e^2 and σ_u^2 are also depicted.

To quantitatively compare the change in the target, disturbance and remnant contributions due to preview and motion

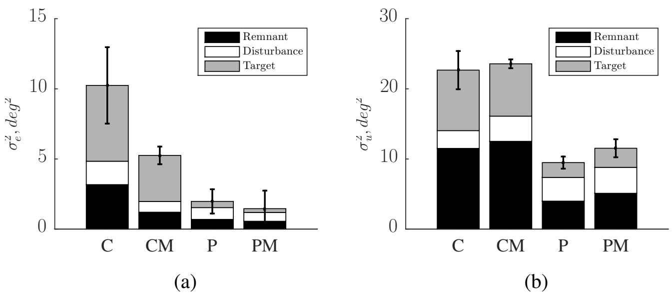

Fig. 10: Variance of the error (a) and control output (b)

feedback, the percentage change in variance is presented in Tables IV and V.

TABLE IV: MOTION AND PREVIEW EFFECTS ON THE ERROR VARIANCE

Frequencies	Motion Effect		Preview Effect	
	Compensatory	Preview	No Motion	Motion
Total	-49%	-26%	-81%	-72%
Remnant	-62%	-19%	-78%	-53%
Disturbance	-54%	-25%	-50%	-18%
Target	-39%	-39%	-92%	-92%

TABLE V: MOTION AND PREVIEW EFFECTS ON THE CONTROL OUTPUT VARIANCE

Frequencies	Motion Effect		Preview Effect	
	Compensatory	Preview	No Motion	Motion
Total	+4%	+22%	-58%	-51%
Remnant	+9%	+28%	-65%	-59%
Disturbance	+42%	+9%	+33%	+3%
Target	-13%	+29%	-75%	-64%

A statistical test is performed in order to further understand how significant are the effects of the different displays and motion feedback for the error and control output variance.

When analyzing the error variances, there is a significant difference in performance for the target, remnant and disturbance contributions, both for motion and displays. This suggests that the extra information provided to the human controller effectively allows to control the system with a smaller error.

Preview yields a significant improvement in target performance, see Table VI. This is most visible in the target frequencies, with a reduction in the error of 92%. With preview, humans can see the future target and anticipate its upcoming changes. There is a significant effect of the applied display variation for the target, disturbance and remnant frequencies on the tracking performance, which shows that preview information allows the human controller to improve both its target-tracking and disturbance-rejection performance.

TABLE VI: TRACKING PERFORMANCE AND CONTROL ACTIVITY ANOVA RESULTS [1]

		error, e			control output, u		
		df	F	sig.	df	F	sig.
σ^2	motion	(1,7)	12.033	*	(1,7)	0.220	-
	display	(1,7)	44.264	**	(1,7)	14.559	**
	mot.*disp.	(1,7)	13.107	**	(1,7)	0.055	-
σ_t^2	motion	(1,7)	15.265	**	(1,7)	0.114	-
	display	(1,7)	89.992	**	(1,7)	84.244	**
	mot.*disp.	(1,7)	18.795	**	(1,7)	2.074	-
σ_d^2	motion	(1,7)	30.030	**	(1,7)	2.956	-
	display	(1,7)	35.639	**	(1,7)	0.805	-
	mot.*disp.	(1,7)	17.369	**	(1,7)	1.762	-
σ_n^2	motion	(1,7)	6.111	*	(1,7)	0.271	-
	display	(1,7)	12.342	*	(1,7)	9.414	*
	mot.*disp.	(1,7)	7.500	*	(1,7)	0.001	-

[1]The symbol - stands for not significant result (p>0.05), * for significant result (p<0.05) and ** for highly significant result (p<0.01)

Motion feedback also has a significant effect on tracking performance, which can be seen for all frequencies. This effect can be seen both for compensatory and preview displays. The motion effect exists for both displays, even though it is smaller in percentage for the preview display. This is can clearly be seen in Table IV, and is also seen in the statistical results as a significant interaction of motion and display for target, disturbance and remnant frequencies tracking performance. This suggests human controllers indeed use motion feedback in preview tracking.

Regarding control activity, the statistical analysis indicates that only the display has a significant effect on the target frequencies. Because human controllers can distinguish between the target and disturbance signals on the preview display (and not on the compensatory display), they respond more linearly (less remnant) and they choose to respond less aggressively to the target signal. Figure 10. When preview is provided, without motion, there is a 58% decrease in the control activity, and a 33% increase in the disturbance control activity, which is not significant.

Motion feedback does not have a significant effect on the control activity. This can also be clearly seen in Figure 10 and Table V, in which the change in control activity variance between the motion and no motion condition are very small.

B. Coherence

The average coherence for each condition is shown in Figure 11 for the target frequencies and in Figure 12 for the disturbance frequencies.

It is clear that all results are very close to 1, which validates the use of a quasi-linear model for the human. These results are 10 to 20 % higher, depending on the frequency, than what was found in previous preview tracking experiments [22], [11], which can be explained by the amplitude filter used in this experiment. The use of an amplitude filter reduces the power of the high frequencies of the signal, which makes the task

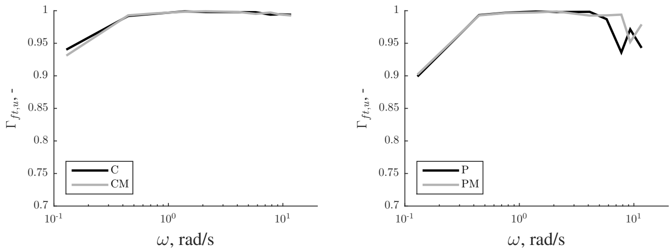

(a) (b)

Fig. 11: Coherence between the target and control output signals, for the compensatory (a) and preview (b) tasks

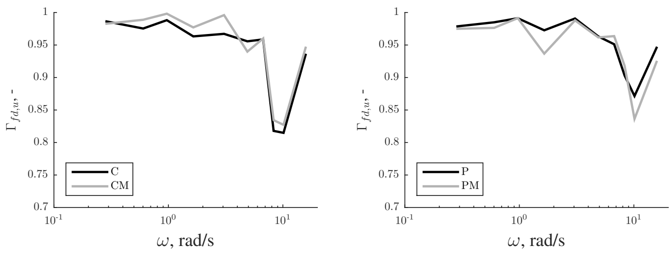

(a) (b)

Fig. 12: Coherence between the disturbance and control output signals, for the compensatory (a) and preview (b) tasks

easier for the human controller. It should also be noted that the disturbance coherence at the higher frequencies is smaller than the target coherence.

C. Crossover Frequency and Phase Margin

The crossover frequencies and phase margins are shown in Figures 13 and 14. In each figure, the results for each subject are presented, along with the mean of all subjects and the 95% confidence intervals of the means.

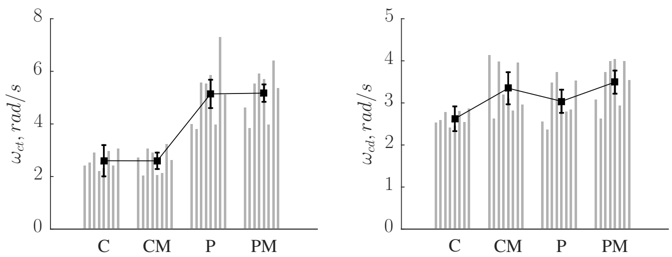

(a) (b)

Fig. 13: Target (a) and disturbance (b) crossover frequency

Figure 13 and 14 shows clear effect of both preview and motion feedback. On the one hand, preview significantly increases the target crossover frequency and phase margin. For target-tracking, preview allows the human to become more stable (increased phase margin), due to the ability to see the future target. The negative time delay present in the preview task provide phase lead to the human controller, which makes the system more stable. On the other hand, motion significantly increases the disturbance crossover frequency, as the disturbance task is easier for the human controller when using motion feedback. It should also be noted that there is an increase in the target crossover frequency when motion is added for the preview task, which is an indicator that motion feedback makes the task easier for the human controller. Neither motion feedback nor preview have a clear contribution to the disturbance phase margin, as can be seen in Figure 14(b), and indeed both effects are not significant, as seen in Table VII.

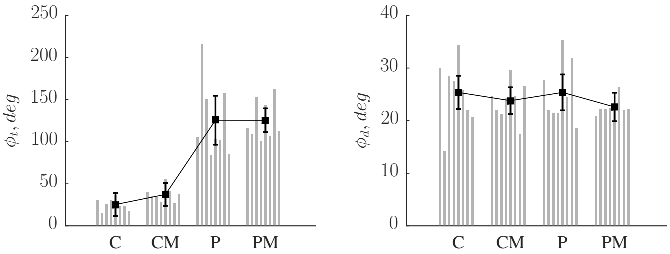

(a) (b)

Fig. 14: Target (a) and disturbance (b) phase margin

TABLE VII: CROSSOVER FREQUENCY AND PHASE MARGIN ANOVA RESULTS [2]

		target			disturbance		
		df	F	sig.	df	F	sig.
	motion	(1,7)	1.487	-	(1,7)	12.126	*
ω_c	display	(1,7)	39.044	**	(1,7)	2.401	-
	mot. * disp.	(1,7)	3.195	-	(1,7)	1.902	-
	motion	(1,7)	0.031	-	(1,7)	0	-
ϕ_m	display	(1,7)	82.872	**	(1,7)	1.079	-
	mot. * disp.	(1,7)	1.320	-	(1,7)	1.217	-

[2]The symbol - stands for not significant result (p>0.05), * for significant result (p<0.05) and ** for highly significant result (p<0.01)

D. Human Controller Describing Functions

Using the Black-Box identification method described in Section IV-H, the human controller describing functions can be identified. The resulting Bode plots are shown in Figures 15-18 for subject 8. This subject is used as a representative example, as there is good correspondence between the Fourier Coefficients (shown as black dots) and the model fit (shown as a line).

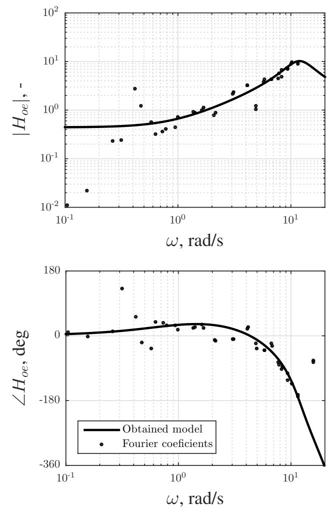

Fig. 15: Frequency response function for the compensatory task without motion feedback (subject 8)

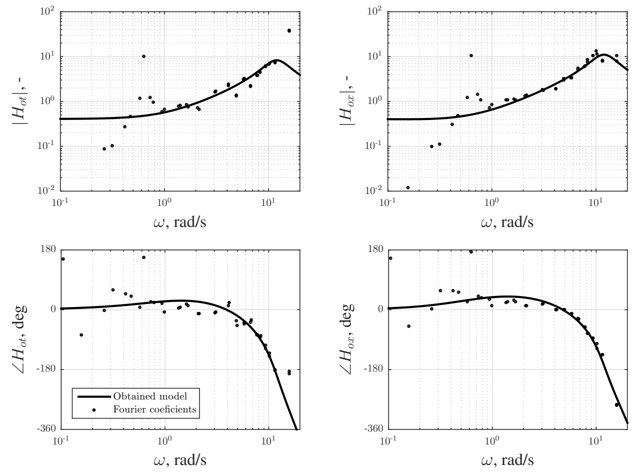

Fig. 16: Frequency response function for the compensatory task with motion feedback (subject 8)

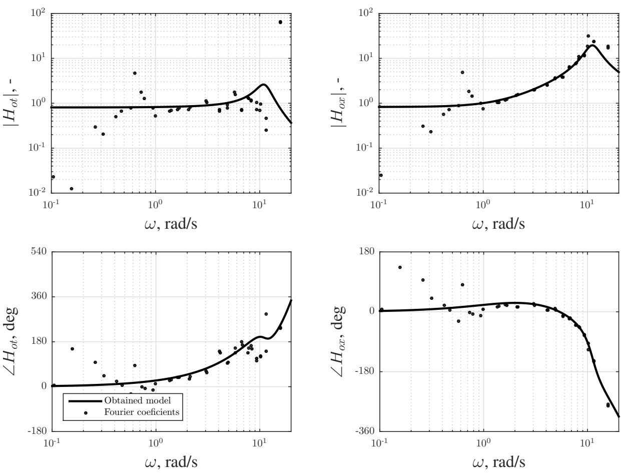

Fig. 17: Frequency response function for the preview task without motion feedback (subject 8)

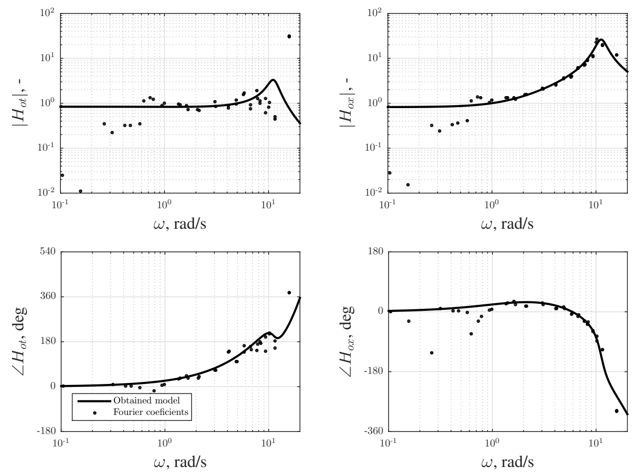

Fig. 18: Frequency response function for the preview task with motion feedback (subject 8)

E. Model comparison

Given the similarity between the models, it was decided to test both the original preview model proposed by van der El et. al [22] and the proposed model for the preview with motion feedback condition. Both models were fitted to the results of the preview with motion feedback condition (PM), in order to understand if the addition of the motion channel causes a significant difference in the Variance Accounted For, the frequency response function, or the parameters of the model. The obtained frequency response functions for both models are presented in Figure 19.

It can be seen in Figure 19 that there is not a significant difference between the two models. The visual channel of the van der El model is able to successfully model the entire response, with only a small change in the Variance Accounted For. The average model parameters are displayed in Table VIII, along with the P results for reference.

TABLE VIII: AVERAGE PARAMETER COMPARISON

	$K_e, -$	$T_{L,e}, s$	$\omega_{nms}, rad/s$	$\zeta_{nms}, -$	τ_v, s
P	0.52	1.14	11.40	0.17	0.24
PM van der El	0.87	0.68	11.95	0.21	0.18
PM Proposed	0.73	0.39	12.77	0.25	0.12
	$K_f, -$	$T_{l,f}, s$	τ_f, s	$K_m, -$	τ_m, s
P	0.92	0.57	0.77	-	-
PM van der El	1.00	0.70	0.68	-	-
PM Proposed	0.93	0.14	0.57	0.28	0.29

For the visual time delay τ_v and the lead time constant $T_{L,e}$, the notably lower values in the proposed model are caused by the interaction with the motion feedback path, as described in Section II-C. The far-viewpoint time constant $T_{l,f}$ seems to

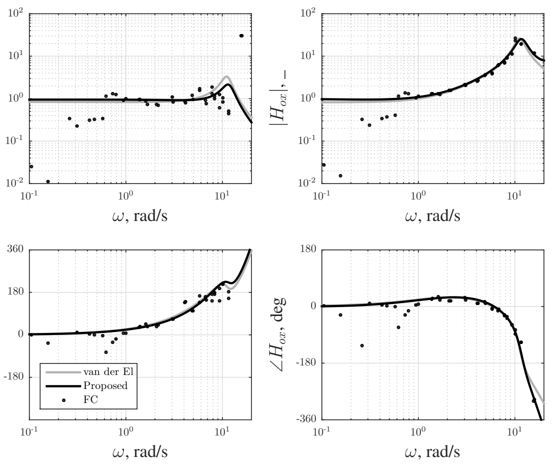

(a)

Fig. 19: Frequency response functions for Subject 8, fitted for the van der El model (VAF=92.38%) and the proposed model including motion feedback (VAF=92.79%).

be the most affected by the change in these parameters.

The visual channel is then able to fully model the response, which is due to the similar function performed by the visual and motion channels in the proposed model. This fact reveals some ambiguity in the proposed model: even though it can fit the human response, it is an overdetermined model. The results for tracking performance and crossover frequency show that indeed there is a change in the human controller, but the proposed model does not correctly fit to the data using the identification techniques presented in this paper. We recommend further research on the separation of the motion and visual channels of the human controller, so that they can be uniquely identified and modeled. Considering these facts, the parameter estimation results obtained from the van der El *et. al* model [22], without the motion feedback channel will be used for the PM condition.

F. Human Controller Model Parameters

The model parameters, for the different conditions, can be seen in Figures 20-25. For each condition, the parameters are shown for each subject using gray bars, along with the mean of all subjects and the 95% confidence interval of the mean.

1) Error feedback response parameters: For both the error response gain $K_{e^\star}$ and lead time constant $T_{L,e^\star}$, the effect of motion feedback is similar for compensatory and preview displays. $K_{e^\star}$ increases when motion feedback is added, as the human responds more aggressively to the error. $T_{L,e^\star}$, on the other hand, shows a significant decrease, as the human controller is required to generate less lead in his visual response. These results are consistent with previous work on compensatory tasks [15], [7].

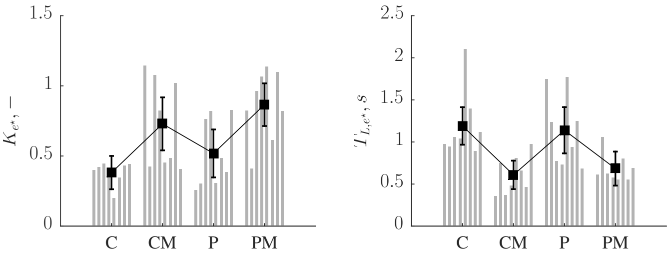

(a) (b)

Fig. 20: Error response gain (a) and lead time constant (b)

2) Neuromuscular system parameters: Regarding the neuromuscular system parameters, motion feedback also has an important effect. There is an increase in the neuromuscular frequency ω_{nms} for both displays (see Figure 21(a)), with a 14% increase in the compensatory case and a 4% increase in the preview case. The increase for the compensatory task is according to what is commonly found in literature, [13], [7]. The neuromuscular damping ζ_{nms} registers a 21% increase for the compensatory case and a 25% increase for the preview case when motion is added.

3) Visual time delay: The visual time delay shows different effects for the compensatory and preview conditions. Using the compensatory display, when motion is added there is a 12% increase in the visual time delay, in line with what was reported in [7]. For the preview conditions, however, when motion is added there is a 24% decrease in the visual time delay.

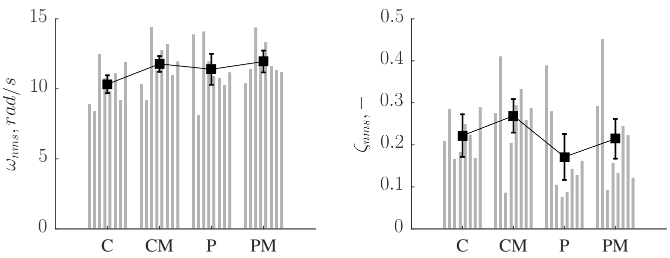

(a) (b)

Fig. 21: Neuromuscular system parameters: natural frequency (a) and damping ratio (b)

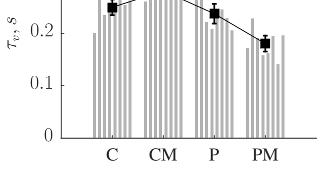

(a)

Fig. 22: Visual time delay

4) Far-viewpoint response parameters: The effect of motion feedback on the far-viewpoint gain K_f is small (see Figure 23(a)). It should also be noted that the parameter is extremely consistent across subjects and essentially a unit gain. The change in the far-viewpoint time-constant $T_{l,f}$ and position τ_f are also small, which suggest that motion feedback doesn't have a substantial effect in the way human controllers use preview.

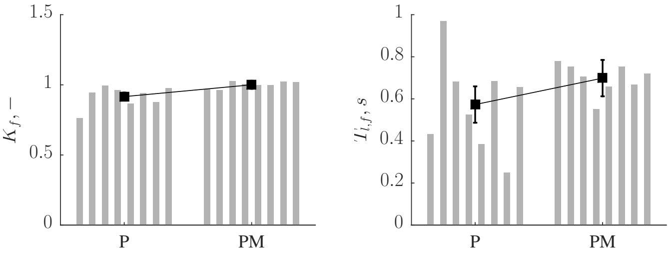

(a) (b)

Fig. 23: Far-viewpoint gain (a) and lead time constant (b)

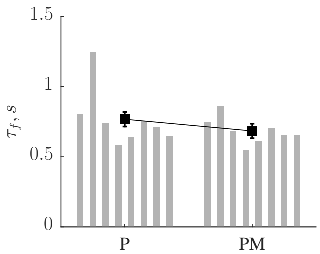

(a)

Fig. 24: Far-viewpoint position

5) Motion feedback parameters: For the compensatory tracking task, both the motion gain K_m and the motion time delay τ_m are consistent with literature results [7].

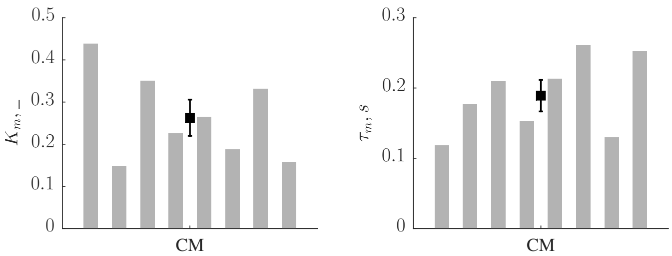

(a) (b)

Fig. 25: Motion parameters: motion gain (a) and motion time delay (b)

G. Variance Accounted For

The obtained Variance Accounted For, shown in Figure 26 is well above 70% for all subjects in all conditions, which suggests the models used are an adequate representation of the human behavior. The proposed model for preview with motion feedback registers the lowest VAF found out of all model fits, with 75%, which is still a high value for this measure. In general, the model fits the experimental data well. The high values for VAFs across conditions are also justified by the fact that the data was averaged in the frequency domain, as in [23].

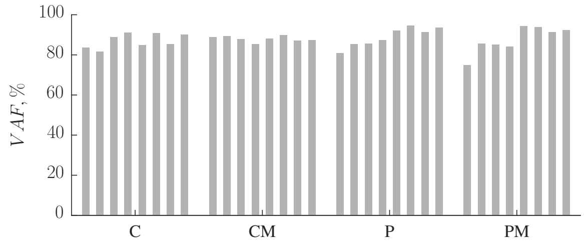

(a)

Fig. 26: Model VAFs per condition and subject

VI. Discussion

In this paper, a human-in-the-loop tracking experiment was performed to study the role of motion feedback in preview tracking tasks in comparison with compensatory tracking.

Motion feedback allows humans to improve their performance in compensatory tracking tasks, which is consistent with many earlier investigations [4], [18], [15], [27], [13], [7], and was also predicted by the offline model simulations. Using motion feedback, humans are able to adapt their behavior, by controlling the system with an higher gain and being required to generate less lead. This result is thus highly consistent with compensatory literature, and confirms Hypothesis I.

When no motion feedback is present, preview allows humans to improve their performance significantly, as predicted by the offline model simulations. The ability to see the future target allows humans to improve tracking performance, which confirms Hypothesis II. Human controllers respond to an internal error, filtered by the far-viewpoint response dynamics, as was found in the work of van der El *et. al* [22].

For preview tracking, the effect of motion is seemingly similar as in compensatory tracking. Motion still allows a significant improvement in performance, and the human adaptation is shown by an increase of the error response gain $K_{e^\star}$ and a decrease of the lead time constant $T_{L,e^\star}$. The results are the opposite as predicted by offline model simulations, in which motion feedback caused a performance degradation for preview tasks. It can be seen, however, that the reduction in error at the disturbance frequencies is found in the experiment results, partially confirming Hypothesis III. However, we were not able to prove the use of the additional motion channel H_{om}, due to the ambiguity of the proposed model. The predicted increase in error for the target frequencies was not found, a difference that may well be explained by human adaptation, which was not taken into account in the offline model simulations. Motion does not cause a change in the way human controllers use preview parameters, with the far-viewpoint parameters registering only small changes. Control activity is not significantly affected by the availability of motion feedback, as found for the compensatory case.

The offline model simulations which were performed for the prediction of the experimental results were not accurate. The adaptation of the human controller, not taken into account for the model simulations, was likely an important factor, and the variation of only one parameter did not yield accurate predictions.

Regarding the parameter estimation results, even though the proposed model is able to fit the data correctly, it is ambiguous regarding the parameters on the motion feedback loop. Based on this fact, we recommend further research that is able to clearly separate the visual and motion channels.

This paper successfully showed for the first time the role of motion feedback on preview tracking tasks: when preview information is available, human controllers are still able to adapt their control behavior and improve tracking performance, without a substantial change in control activity.

VII. Conclusion

This paper studied the effect of yaw motion feedback on human control behavior in preview tracking tasks. We proposed a new quasi-linear human controller model for visual and preview tracking tasks with an additional motion feedback channel. First, the model was tested in an offline model simulation to predict the effects of motion feedback in compensatory and preview tracking tasks. Second, a human-in-the-loop tracking experiment was performed in the SIMONA Research Simulator at TU Delft to validate the offline predictions. Results show that motion feedback helps to improve performance similarly in preview tasks, as it does in compensatory tasks, with an increase in the error response gain and a reduction in the lead time constant. The target crossover frequency and phase margin are mostly influenced by preview, while the disturbance crossover frequency is mostly influenced by the motion feedback. With this research, the effects of motion feedback in preview were studied for the first time, effectively allowing to bridge the knowledge gap between compensatory tasks with motion and preview tasks, by showing that human controllers use motion feedback in preview tracking to adapt their control behavior.

References

[1] H. J. Damveld, G. C. Beerens, M. M. van Paassen, and M. Mulder, "Design of Forcing Functions for the Identification of Human Control Behavior," *Journal of Guidance, Control, and Dynamics*, vol. 33, no. 4, pp. 1064–1081, Jul. 2010.

[2] K. Guo and H. Guan, "Modelling of Driver/Vehicle Directional Control System," *Vehicle System Dynamics*, vol. 22, no. 3, pp. 141–184, 1993.

[3] R. J. A. W. Hosman, "Pilot's Perception and Control of Aircraft Motions," Ph.D. dissertation, Delft University of Technology, Faculty of Aerospace Engineering, 1996.

[4] R. J. A. W. Hosman and J. C. van der Vaart, "Effects of Vestibular and Visual Motion Perception on Task Performance," *Acta Psychologica*, vol. 48, pp. 271–287, 1981.

[5] K. Ito and M. Ito, "Tracking behavior of human operators in preview control systems," *Electrical Engineering in Japan*, vol. 95, no. 1, pp. 120–127, 1975.

[6] H. R. Jex, R. E. Magdaleno, and A. M. Junker, "Roll Tracking Effects of G-vector Tilt and Various Types of Motion Washout," in *Proceedings of the Fourteenth Annual Conference on Manual Control*, 1978, pp. 463–502.

[7] T. Lu, D. M. Pool, M. M. van Paassen, and M. Mulder, "Use of Simulator Motion Feedback for Different Classes of Vehicle Dynamics in Manual Control Tasks," in *Proceedings of the 5th CEAS Air & Space Conference, Delft, The Netherlands*, no. 52, Sep. 2015.

[8] C. C. MacAdam, "Understanding and Modeling the Human Driver," *Vehicle System Dynamics*, vol. 40, no. 1-3, pp. 101–143, Jan. 2003.

[9] D. McRuer and H. Jex, "A Review of Quasi-Linear Pilot Models," *IEEE Transactions on Human Factors in Electronics*, vol. 8, no. 3, pp. 231–249, 1967.

[10] F. M. Nieuwenhuizen, P. M. T. Zaal, M. Mulder, M. M. van Paassen, and J. A. Mulder, "Modeling Human Multichannel Perception and Control Using Linear Time-Invariant Models," *Journal of Guidance, Control, and Dynamics*, vol. 31, no. 4, pp. 999–1013, July-August 2008.

[11] S. Padmos, K. van der El, D. M. Pool, H. J. Damveld, M. M. van Paassen, and M. Mulder, "The effect of preview time on human control behavior in rate and acceleration tracking tasks," *In preparation*, 2016.

[12] D. M. Pool, "Objective Evaluation of Flight Simulator Motion Cueing Fidelity Through a Cybernetic Approach," Ph.D. dissertation, Delft University of Technology, Faculty of Aerospace Engineering, Sep. 2012.

[13] D. M. Pool, H. J. Damveld, M. M. van Paassen, and M. Mulder, "Tuning Models of Pilot Tracking Behavior for a Specific Simulator Motion Cueing Setting," in *Proceedings of the AIAA Modeling and Simulation Technologies Conference, Portland, Oregon, Aug. 8-11*, no. AIAA-2011-6322, 2011.

[14] D. M. Pool, G. A. Harder, and M. M. van Paassen, "Effects of Simulator Motion Feedback on Training of Skill-Based Control Behavior," *Journal of Guidance, Control, and Dynamics*, vol. 39, no. 4, pp. 889–902, 2016.

[15] D. M. Pool, M. Mulder, M. M. van Paassen, and J. C. van der Vaart, "Effects of Peripheral Visual and Physical Motion Cues in Roll-Axis Tracking Tasks," *Journal of Guidance, Control, and Dynamics*, vol. 31, no. 6, pp. 1608–1622, 2008.

[16] D. M. Pool, A. R. Valente Pais, A. M. de Vroome, M. M. van Paassen, and M. Mulder, "Identification of Nonlinear Motion Perception Dynamics Using Time-Domain Pilot Modeling," *Journal of Guidance, Control, and Dynamics*, vol. 35, no. 3, pp. 749–763, May–June 2012.

[17] B. S. Repa, P. M. Leucht, and W. W. Wierwille, "The Influence of Motion Cues on Driver-Vehicle Performance in a Simulator," in *Proceedings of the Seventeenth Annual Conference on Manual Control, Los Angeles (CA)*, Oct. 1981, pp. 157–169.

[18] J. A. Schroeder, "Simulation Motion Effects on Single Axis Compensatory Tracking," in *Proceedings of the AIAA Flight Simulation Technologies Conference, Monterey (CA)*, no. AIAA-1993-3579, 1993, pp. 202–213.

[19] T. B. Sheridan, "Three models of preview control," *IEEE Transactions on Human Factors in Electronics*, vol. 7, no. 2, pp. 91–102, 1966.

[20] J. Steen, H. J. Damveld, R. Happee, M. M. van Paassen, and M. Mulder, "A Review of Visual Driver Models for System Identification Purposes," in *IEEE International Conference on Systems, Man, and Cybernetics (SMC), 2011*, Oct. 2011, pp. 2093 – 2100.

[21] M. Tomizuka and D. E. Whitney, "The Preview Control Problem with Application to Man-Machine System Analysis," in *Proceedings of the Ninth Annual Conference on Manual Control*, 1973, pp. 429–441.

[22] K. van der El, D. M. Pool, H. J. Damveld, M. M. van Paassen, and M. Mulder, "An Empirical Human Controller Model for Preview Tracking Tasks," *IEEE Transactions on Cybernetics*, 2015.

[23] K. van der El, D. M. Pool, M. M. van Paassen, and M. Mulder, "How Human Controllers use Preview to Improve Target-Tracking Performance," *IEEE Transactions on Cybernetics*, 2016.

[24] M. M. van Paassen and M. Mulder, "Identification of Human Operator Control Behaviour in Multiple-Loop Tracking Tasks," in *Proceedings of the Seventh IFAC/IFIP/IFORS/IEA Symposium on Analysis, Design and Evaluation of Man-Machine Systems, Kyoto Japan*. Pergamon, 1998, pp. 515–520.

[25] M. C. Vos, D. M. Pool, H. J. Damveld, M. M. van Paassen, and M. Mulder, "Identification of Multimodal Control Behavior in Pursuit Tracking Tasks," in *Proceedings of the 2014 IEEE International Conference on Systems, Man, and Cybernetics, San Diego (CA)*, Oct. 2014, pp. 69–74.

[26] P. M. T. Zaal, D. M. Pool, Q. P. Chu, M. M. van Paassen, M. Mulder, and J. A. Mulder, "Modeling Human Multimodal Perception and Control Using Genetic Maximum Likelihood Estimation," *Journal of Guidance, Control, and Dynamics*, vol. 32, no. 4, pp. 1089–1099, 2009.

[27] P. M. T. Zaal, D. M. Pool, J. de Bruin, M. Mulder, and M. M. van Paassen, "Use of Pitch and Heave Motion Cues in a Pitch Control Task," *Journal of Guidance, Control, and Dynamics*, vol. 32, no. 2, pp. 366–377, 2009.

Part II

Book of Appendices

Appendix A

Experiment Briefing

The following pages contain the experiment briefing that was handed to the test subjects. This document contains all the information the subjects were required to know prior to starting the experiment. The briefing starts with a small description of the experiment and its objectives. Then it explains the control task to be performed and the experimental apparatus and procedure. The briefing is concluded by the description of the rights of the participant.

SIMONA Research Simulator Experiment Briefing

Role of Motion Feedback on Preview Tracking Tasks

In this experiment, we aim at finding what is the effect of motion feedback in a preview tracking task. The effects of motion in compensatory tasks were studied in the past, and we intend to extend that knowledge to preview tasks. For the experiment, a preview display inside the SIMONA Research Simulation Cockpit will be used, presenting both compensatory and preview displays, with and without motion feedback.

A-1 Objectives

The goal of this experiment is to understand how humans use motion feedback for a preview tracking task. On the one hand, effect of motion feedback in compensatory tasks is widely known and studied. On the other hand, previous research at the Faculty of Aerospace Engineering was able to obtain a model for preview tracking tasks. The current experiment aims to connect these two pieces of knowledge, by understanding how motion influences the preview task.

A-2 Control task

The control task in this experiment is a combined disturbance-rejection and target-following task, as can be seen in Figure A-1. Depending on the condition, the task will be performed with compensatory or preview displays, see Figure C-5. The compensatory display (Fig. 2 (a)) presents a cross with the current tracking error, and a fixed circle in the center, representing the "crosshair". Your objective is to reduce the error, by placing the circle over the cross as accurately as possible. The preview display (Fig 2 (b)) shows a moving circle which represents the controlled element output. Two seconds of preview will be shown, displaying how the target will move for that period of time, represented by a curved line. The current target position is the bottom of the preview line. The error can be deduced by the difference between x and f_t. Both displays have an inside-out representation.

Your objective is to track the target, following the visual f_t signal. The output x is, for the motion case, the yaw rotation of the simulator. This output will be perturbed by the disturbance signal f_d.

A-3 Experimental apparatus

In this experiment, the SIMONA Research Simulator will be used. You will be seated on the right seat of the simulator cockpit, and use a side-stick to your right to provide the control input, by moving the stick to the left and right. The task will be presented on the primary flight display, in black background with green lines. For the motion case, the motion cue will be the yaw rotation of the simulator. All other motion cues are inactive.

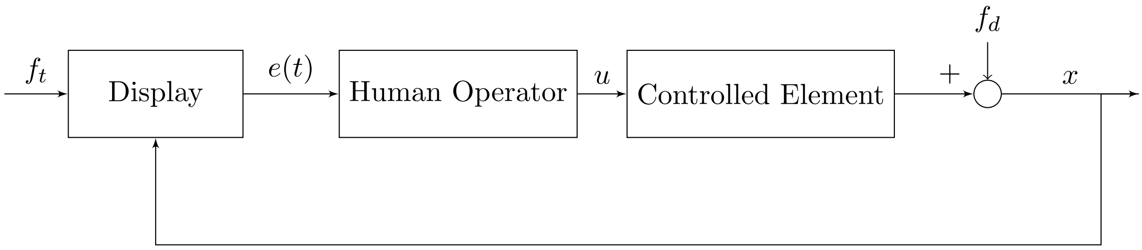

Figure A-1: Block diagram of the combined target-tracking and disturbance rejection task

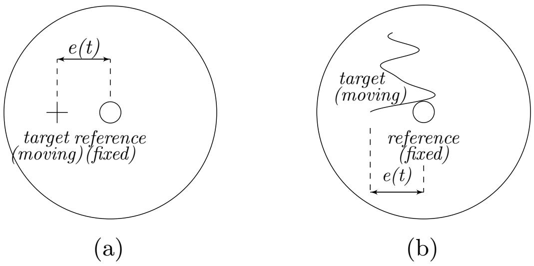

Figure A-2: The compensatory (a) and preview display (b)

A-4 Experimental conditions

The conditions will include two different displays and two different motion conditions. The displays will compensatory and preview, as described before. Regarding the motion feedback, there will be conditions without motion feedback, and conditions with yaw rotation of the simulator cockpit. This yields a total of four experimental conditions: compensatory without motion, compensatory with motion, preview without motion and preview with motion.

A-5 Experimental procedure

The experiment will consist of two main phases: a familiarization and a measurement phase. During the familiarization phase, you will have the time to get used to the displays, control task and motion feedback by performing a limited number of runs of each condition. During the training/measurement phase, the experimenter will track your performance, and after it is sufficiently stable, the actual measurement will start. In total, 8-10 runs are expected for each condition.

Figure A-3: SIMONA Research Simulator

The experimenter will report your performance after each run, using the root mean square of the error between the target and your position. A lower value indicates a better performance.

The four experimental conditions will be tested in a random order. Each run will last for two minutes, and each condition is expected to take around 30 minutes. There will be breaks between conditions in order to avoid fatigue. The total experiment time is expected to be around 3 hours.

A-6 Your rights

Your participation in this experiment is voluntary, and you can terminate it at any time, before or during the experiment.

The data collected in this experiment is anonymous and confidential. The treatment and presentation of the data will be done in a way so that only the experimenter can link the results to the participants, and all participants will remain anonymous. Your participation means that you allow the data to be published.

In order to confirm that you agree and understand all of the above, you will be asked to sign an informed consent form before you start the experiment.

Appendix B

Latin-Square Experimental Design

The experiment performed in this report was a human-in-the-loop experiment on the SIMONA Research Simulator. In such an experiment, human factors play a large role in the results, thanks to the effects of fatigue, motivation, training, and others. In order to avoid confounds in the results, a balanced Latin-square design is used, so that the effect of these factors is minimized in the results.

Table B-1: Balanced Latin-Square Design

Subject	Experimental order			
1	P	PM	C	CM
2	CM	C	PM	P
3	PM	CM	P	C
4	C	P	CM	PM
5	P	PM	C	CM
6	CM	C	PM	P
7	PM	CM	P	C
8	C	P	CM	PM

Appendix C

Choice of Control Variables

In this chapter, the process of choice of the different control variables in the experiment is outlined. The first section details the choice of the forcing function, while the second explains the choice of the display. The motion and controlled element choices are also explained in the following sections. In all of these elements, there was a compromise between similarity with previous literature on visual preview tracking experiments and previous compensatory tracking experiments with motion feedback.

C-1 Forcing Functions

Designing a forcing function for a simulator experiment requires finding a target and disturbance signal that include a number of characteristics. The signals need to be realistic and challenging but not too difficult to follow, as this tires the experiment subjects. Using motion feedback, they also need to be designed in such a way they are comfortable inside the simulator and do not pose a large risk of motion sickness on subjects.

The forcing functions used in previous preview experiments have an amplitude distribution as represented in Figure C-1. This forcing function, used by (El, Pool, Damveld, Paassen, & Mulder, 2015; Padmos et al., 2016) uses double-bands of input frequencies, and an amplitude step of -10dB at the higher frequencies.

When these forcing functions were tested with motion feedback, test subjects weren't able to complete the experiment. The amplitude of the disturbance signal was too high for the task to be comfortable for the subjects using motion feedback. It was also noted that the forcing function included too many high frequencies for it to be realistic. In an effort to mitigate the first problem, it was decided to use a larger amplitude step. Tests were done using a -20db and a -26dB step, but none of these forcing functions were able to be both challenging and comfortable for the subjects.

In previous motion feedback experiments, single-band forcing functions were used. Regarding the amplitudes, instead of using an amplitude step, an amplitude filter is used. A common amplitude filter, found in literature regarding motion feedback, is shown in Equation (C-1).

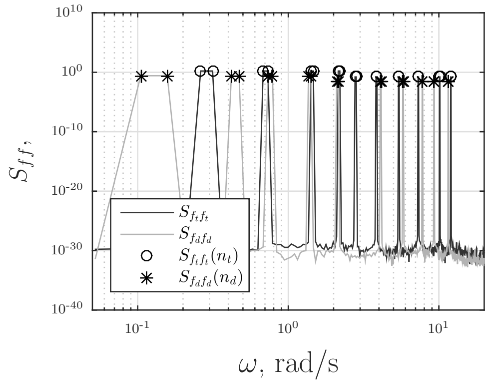

(a)

Figure C-1: Single-sided Power Spectral Density of the forcing function signals in van der El *et. al*

$$H_A(j\omega) = \frac{(1 + 0.1j\omega)^2}{(1 + 0.8j\omega)^2} \tag{C-1}$$

This filter yields forcing functions with a power spectra such as can be seen in Figure C-2 (Zaal, Pool, Bruin, Mulder, & Paassen, 2009).

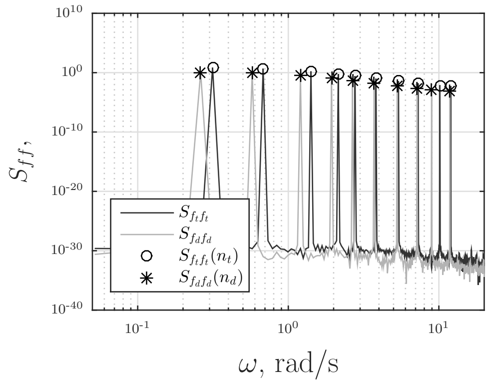

(a)

Figure C-2: Single-sided Power Spectral Density of the forcing function signals in Zaal *et. al*

Combining these two types of forcing functions, a new forcing function was designed for the present experiment. This forcing function includes the double-bands at the same frequencies as in (El et al., 2015) and the amplitude filter used in (Zaal, Pool, Bruin, et al., 2009). The final forcing function power spectra can be seen in Figure C-3. When this forcing function was tested in the simulator, test subjects were able to perform the task, using a comfortable yet challenging forcing function. It should be noted that, since the disturbance signal is inserted before the controlled element, it was filtered with the inverse controlled element dynamics.

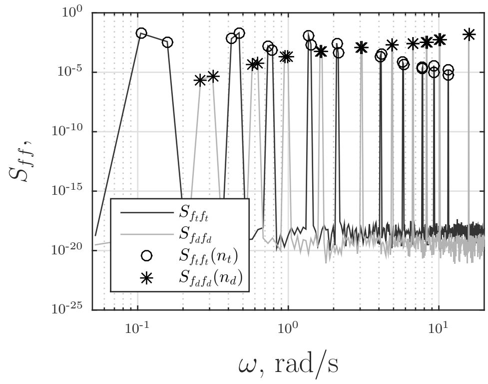

(a)

Figure C-3: Single-sided Power Spectral Density of the forcing function signals

C-2 Display

The preview display used in previous preview tracking experiments is shown in Figure C-4 (El et al., 2015; Padmos et al., 2016).

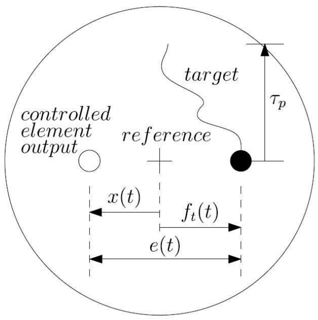

Figure C-4: Preview display used in van der El *et. al*

Since the compensatory display only shows the error, it uses a fixed reference for the controlled element output. With this in mind, it was decided to use an inside-out preview display, with a fixed controlled element output and a moving preview line. The final displays used in the experiment are shown in Figure C-5.

C-3 Motion Feedback

Three different types of motion feedback were initially considered for the experiment: lateral position, yaw and roll. These three types were chosen as they have a direct and easy to understand translation to preview control. Pitch was excluded, since the use of preview for pitch would require a different display from previous experiments, and the adaptation to such a display is not as straightforward as the other motion cues.

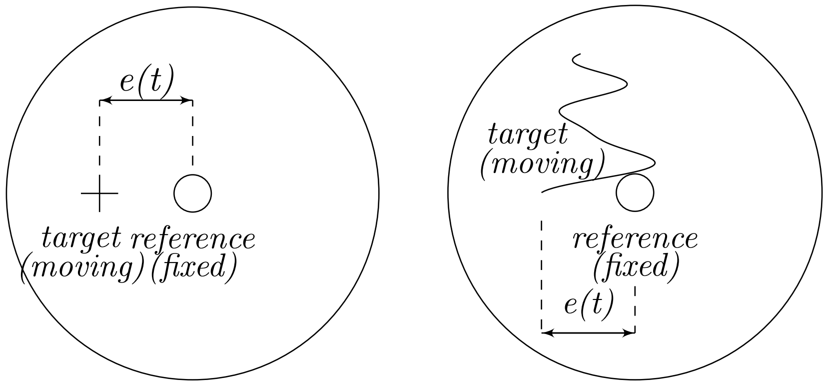

(a) (b)

Figure C-5: The compensatory (a) and preview display (b)

The mental image most commonly associated with preview is that of flying over a road or a river, using a birds-eye view. With this in mind, it was decided to test the control of the lateral position, which is the most straightforward approach to preview with motion feedback. The test runs conducted with this motion cue did not yield good results, as the motion cue was unpleasant to the test subjects. Test subjects felt the disturbance very strongly, and were not able to feel the movement following the target signal.

It was decided to test yaw as a second option for the motion cue. For this type of motion feedback, subjects no longer reported the previous issues, and it was defined the experiment would use yaw as the motion cue.

C-4 Controlled Element

In experiments using motion feedback, two classes of models have been used: models that approximate aircraft dynamics(Zaal, Pool, Bruin, et al., 2009; Pool, Harder, & Paassen, 2016) and simplified systems that approximate realistic dynamics in a certain frequency region, like gain, integrator or double integrator dynamics (Lu, Pool, Paassen, & Mulder, 2015; El et al., 2015).

Considering that previous preview experiments used integrators (El et al., 2015; Padmos et al., 2016), it was decided to use a controlled element of that type in the experiment, in order to reduce the number of different control variables from the present experiment to this literature.

It was also decided to test only the double integrator condition, disregarding gain and single integrator dynamics. In studies such as (Lu et al., 2015), it is found that the motion channel is clearly active for these dynamics, and humans indeed adapt their behavior to the motion feedback. This condition was also studied in preview experiments. It is therefore a controlled element which allows to connect previous studies, and testing only one dynamic also allows to reduce the number of experimental conditions and the experiment time demanded to the subjects.

Appendix D

Coherence Results

In the following pages, the coherence results are presented for each subject. For each of the eight subjects, both target and disturbance coherence are shown, for each of the four conditions. The conditions were paired in order to facilitate comparison between motion and no motion conditions.

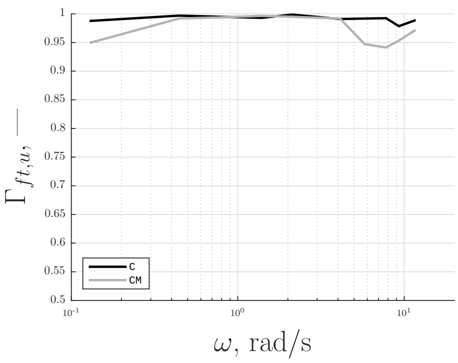

(a)

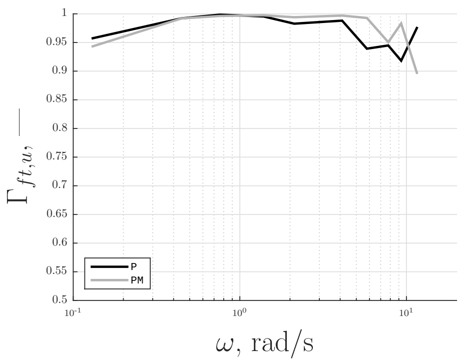

(b)

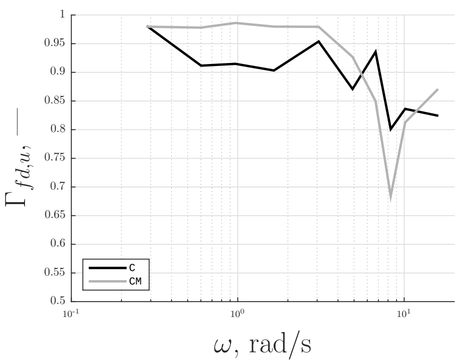

(c)

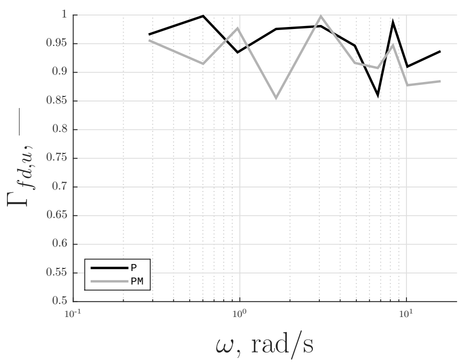

(d)

Figure D-1: Coherence results for Subject 1. Target coherence for compensatory (a) and preview (b) tasks and disturbance coherence for compensatory (c) and preview (d) tasks

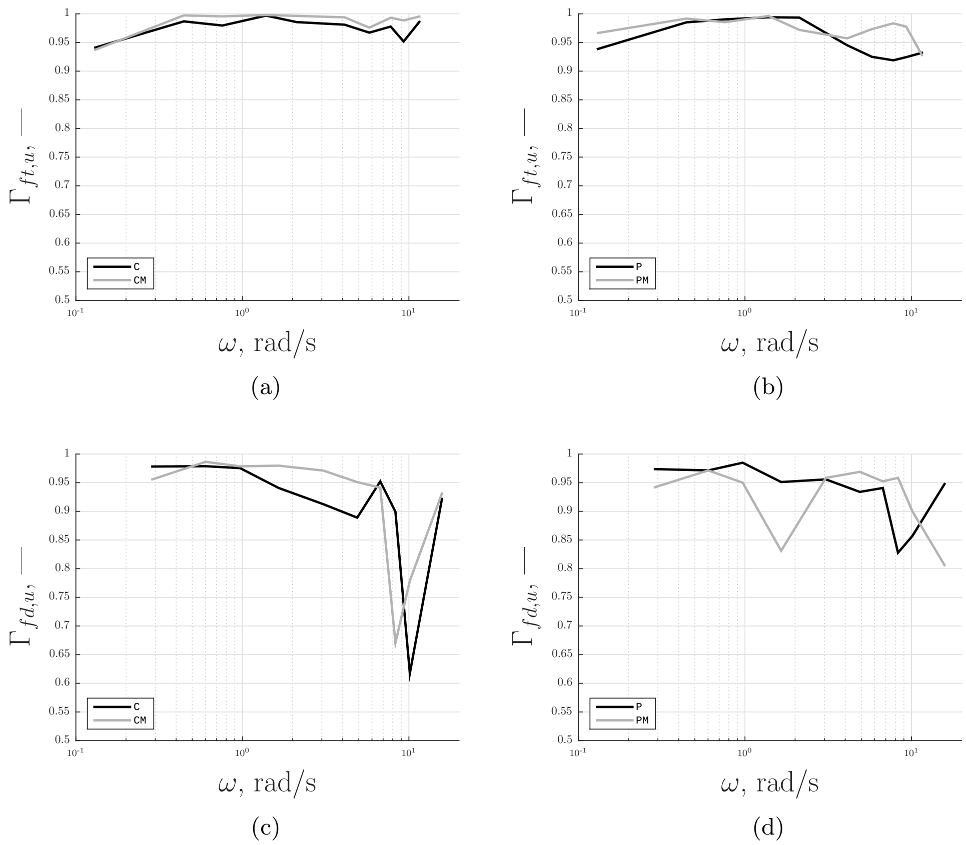

Figure D-2: Coherence results for Subject 2. Target coherence for compensatory (a) and preview (b) tasks and disturbance coherence for compensatory (c) and preview (d) tasks

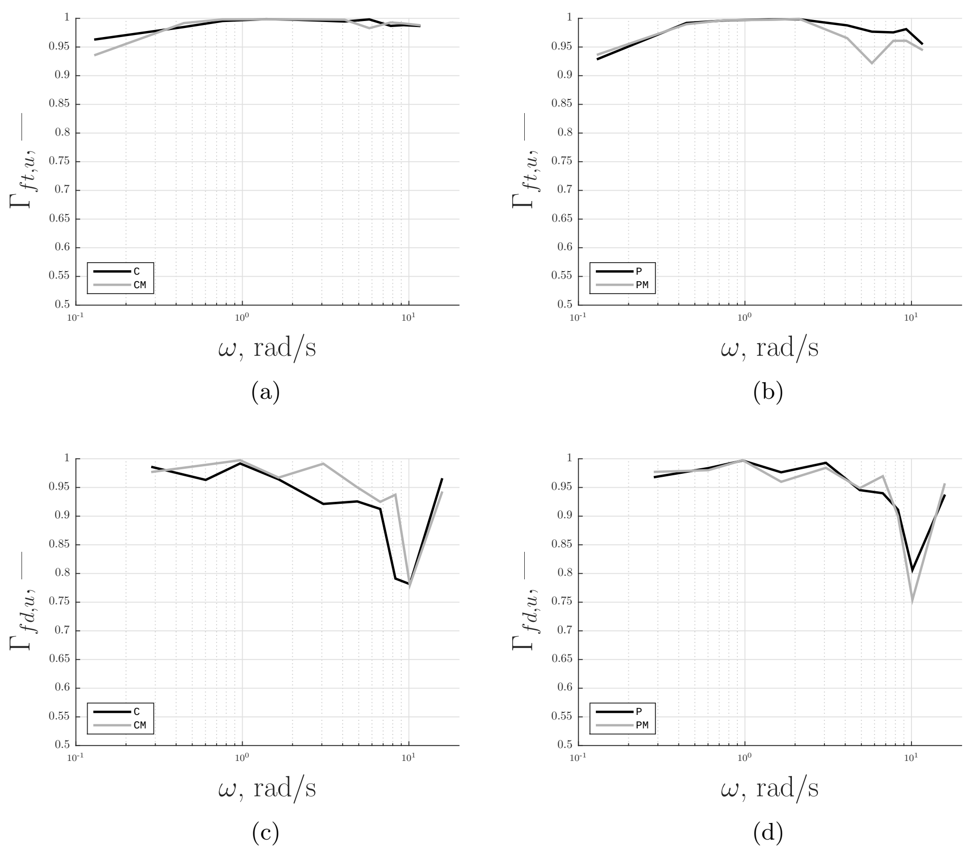

Figure D-3: Coherence results for Subject 3. Target coherence for compensatory (a) and preview (b) tasks and disturbance coherence for compensatory (c) and preview (d) tasks

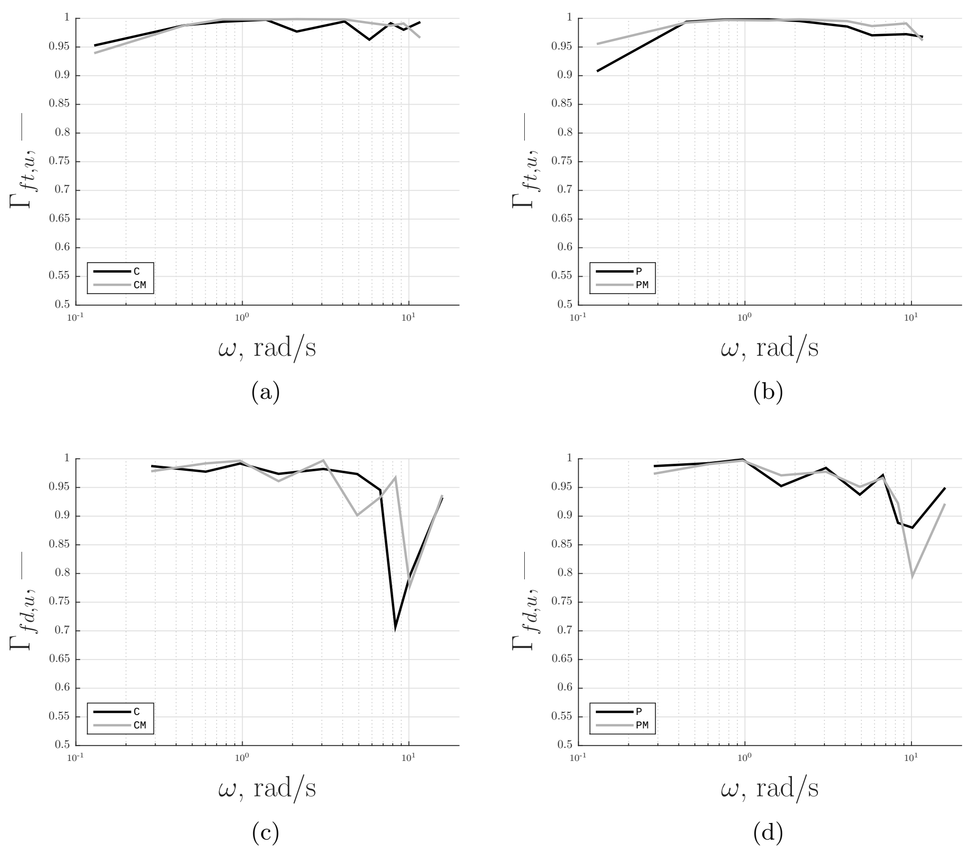

Figure D-4: Coherence results for Subject 4. Target coherence for compensatory (a) and preview (b) tasks and disturbance coherence for compensatory (c) and preview (d) tasks

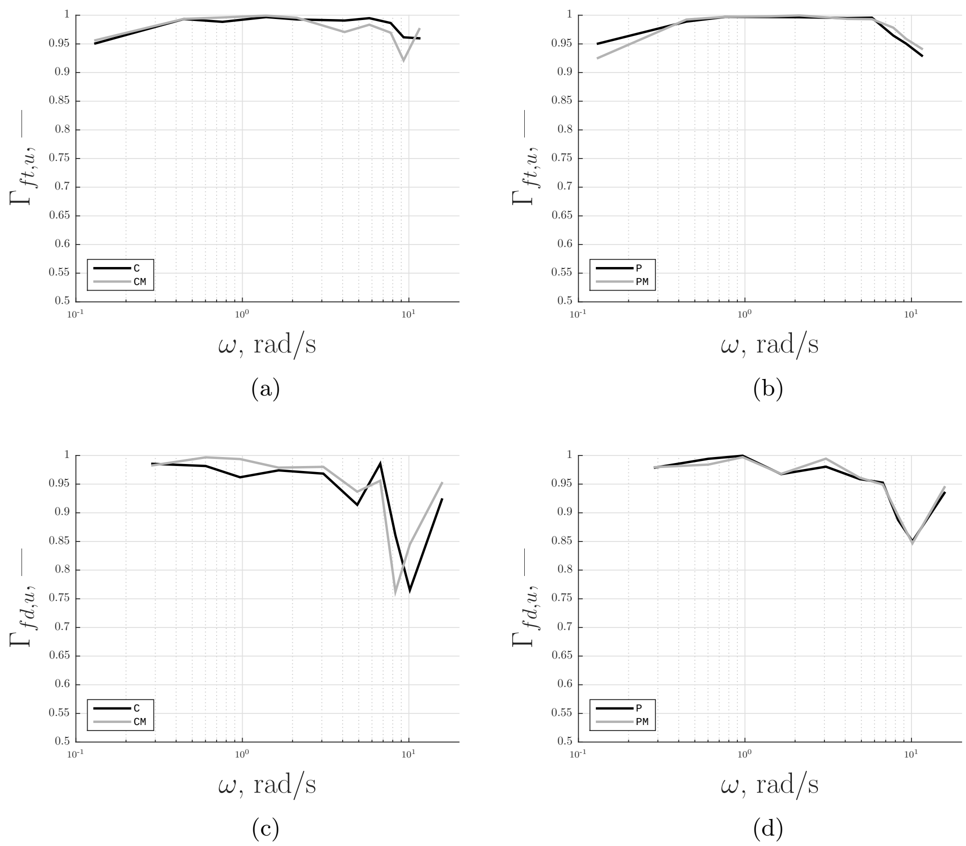

Figure D-5: Coherence results for Subject 5. Target coherence for compensatory (a) and preview (b) tasks and disturbance coherence for compensatory (c) and preview (d) tasks

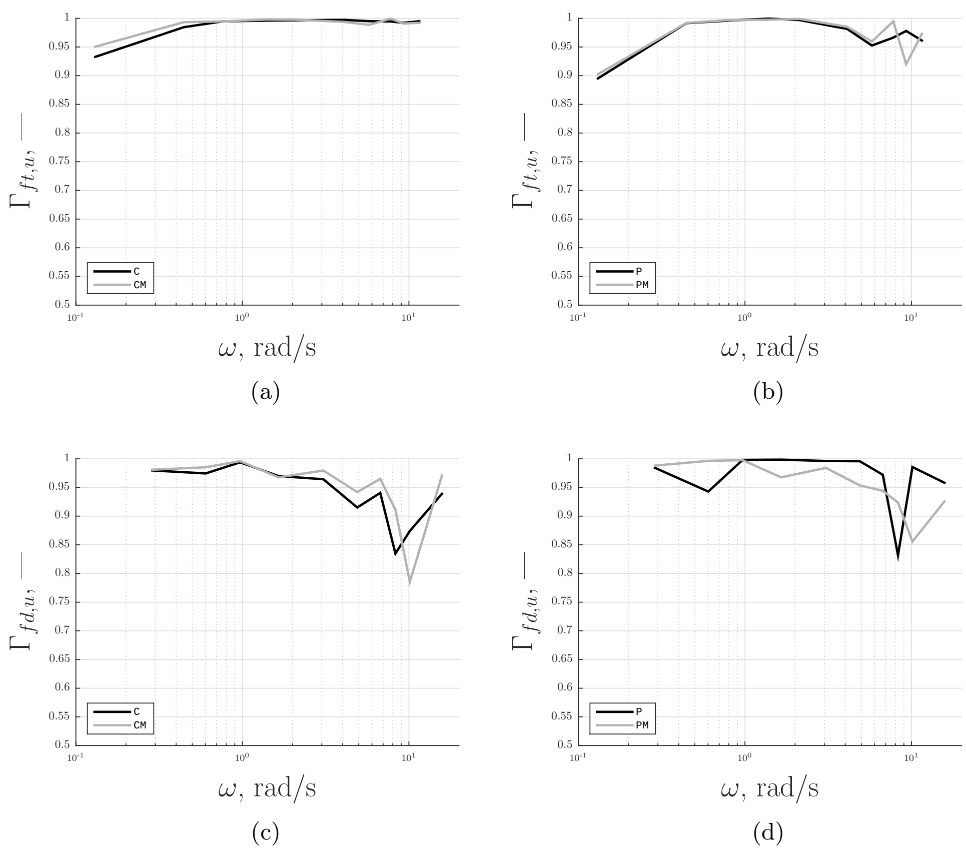

Figure D-6: Coherence results for Subject 6. Target coherence for compensatory (a) and preview (b) tasks and disturbance coherence for compensatory (c) and preview (d) tasks

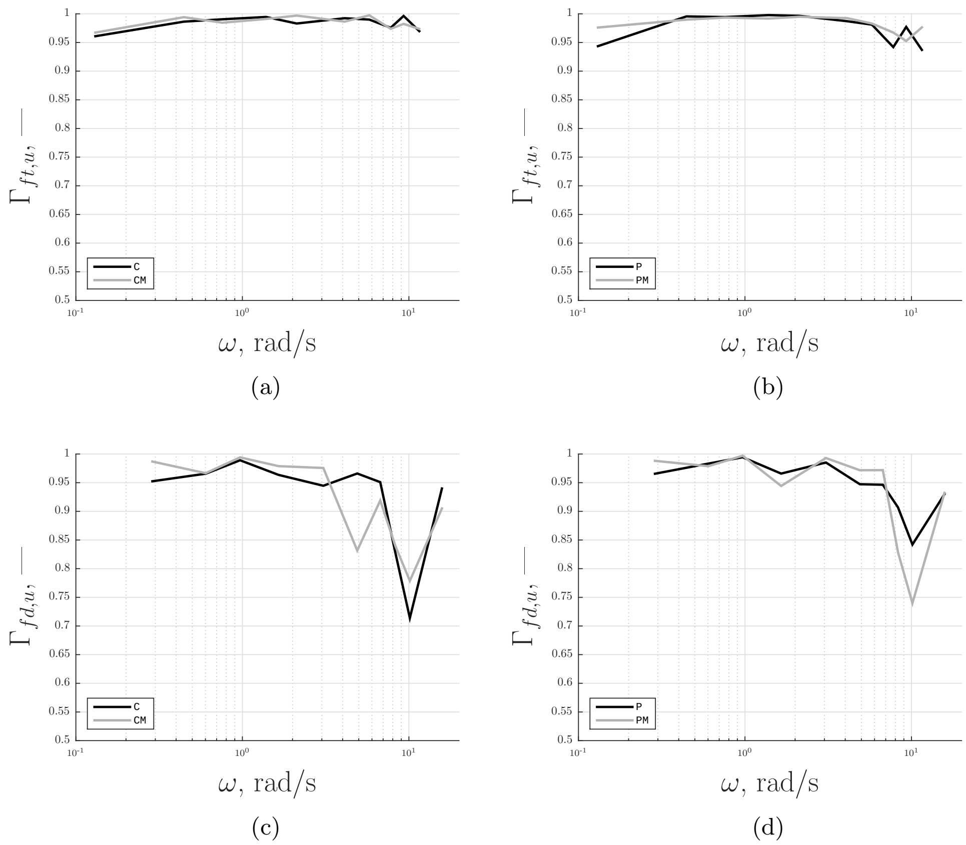

Figure D-7: Coherence results for Subject 7. Target coherence for compensatory (a) and preview (b) tasks and disturbance coherence for compensatory (c) and preview (d) tasks

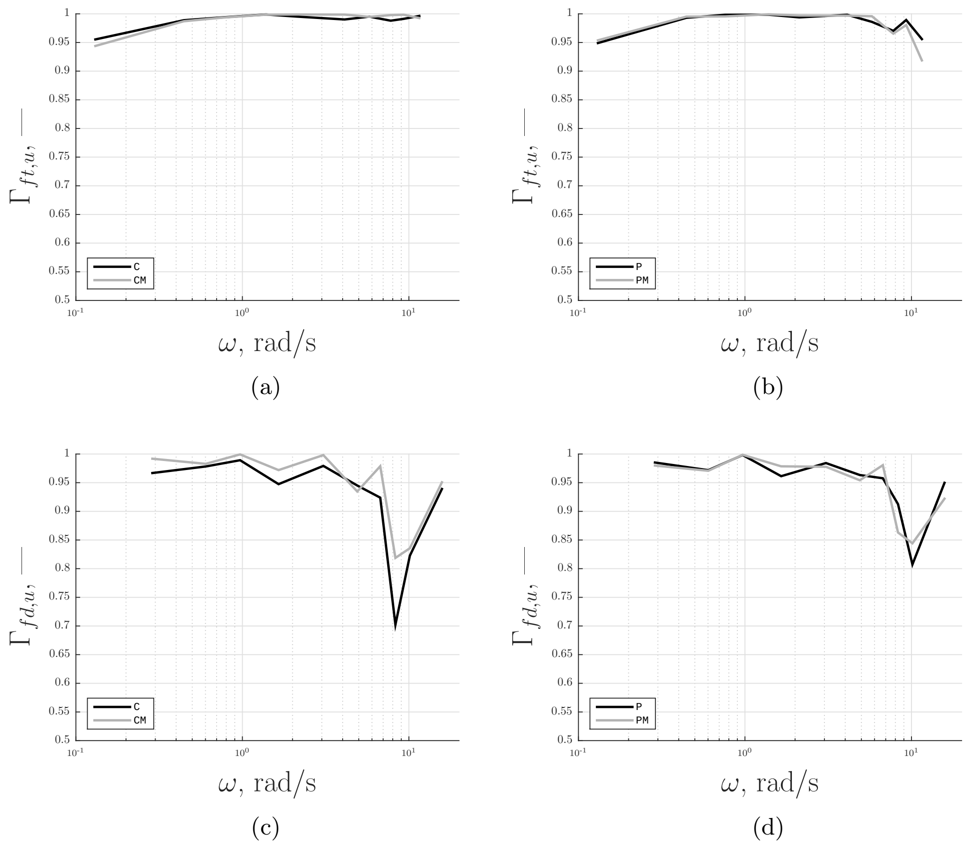

Figure D-8: Coherence results for Subject 8. Target coherence for compensatory (a) and preview (b) tasks and disturbance coherence for compensatory (c) and preview (d) tasks

Appendix E

Variance Results

The variances of the error and control activity were obtained using the integration of the power spectral density. This method allows to separate the contribution of the target, disturbance and remnant frequencies. In the following figures, the contributions of each of these frequencies are shown for each of the eight test subjects are shown as gray bars. The average and 95% confidence interval are shown in black. The total variance split in the different contributions is also shown per subject.

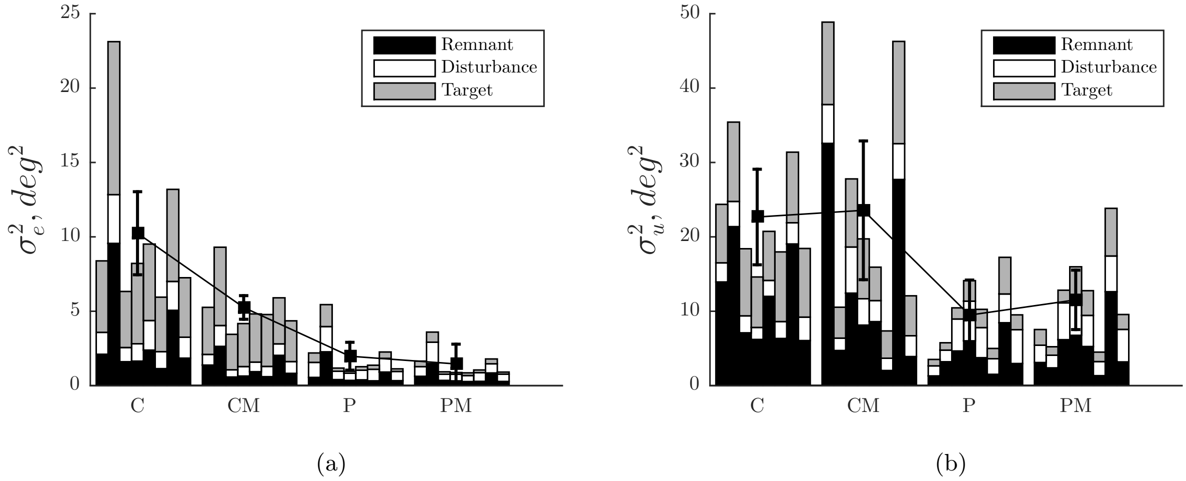

Figure E-1: Variance of the tracking error (a) and control activity (b) for all subjects, split into target, disturbance and remnant frequencies

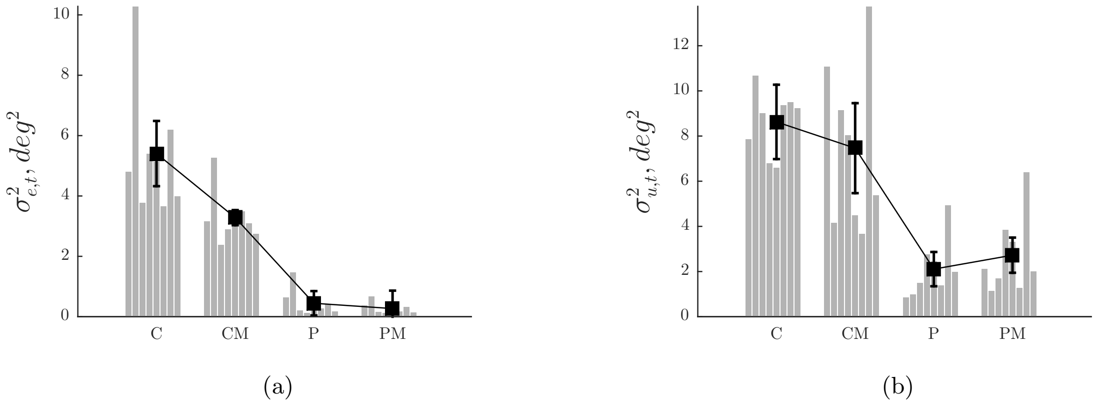

Figure E-2: Variance of the tracking error (a) and control activity (b) for remnant frequencies

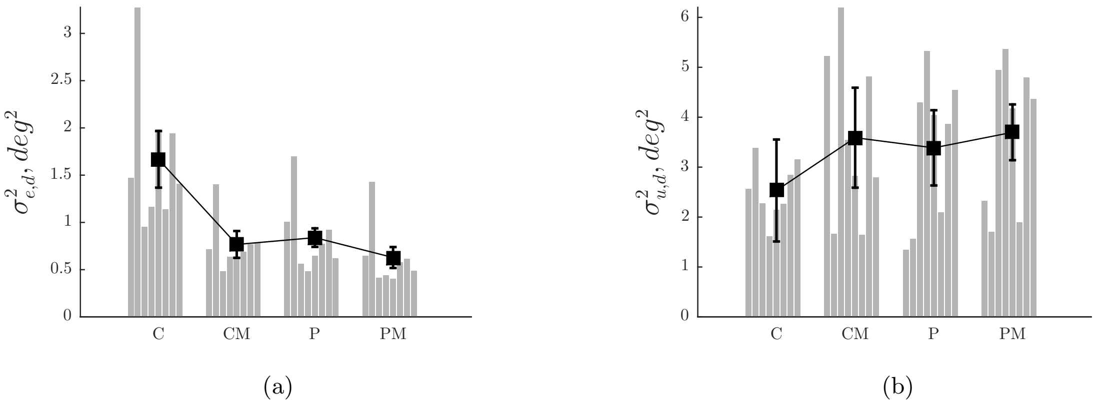

Figure E-3: Variance of the tracking error (a) and control activity (b) for remnant frequencies

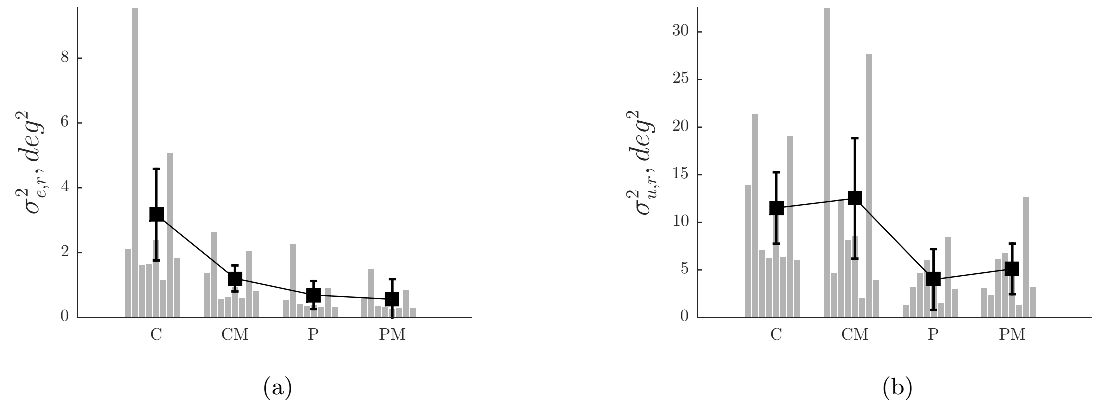

Figure E-4: Variance of the tracking error (a) and control activity (b) for remnant frequencies

Appendix F

Human Controller Describing Functions

The following pages include the human controller frequency response functions for each of the test subjects in each condition. In each figure are displayed both the Fourier Coefficients obtained using the black-box system identification method described in the paper, and the parametric model obtained through parameter estimation.

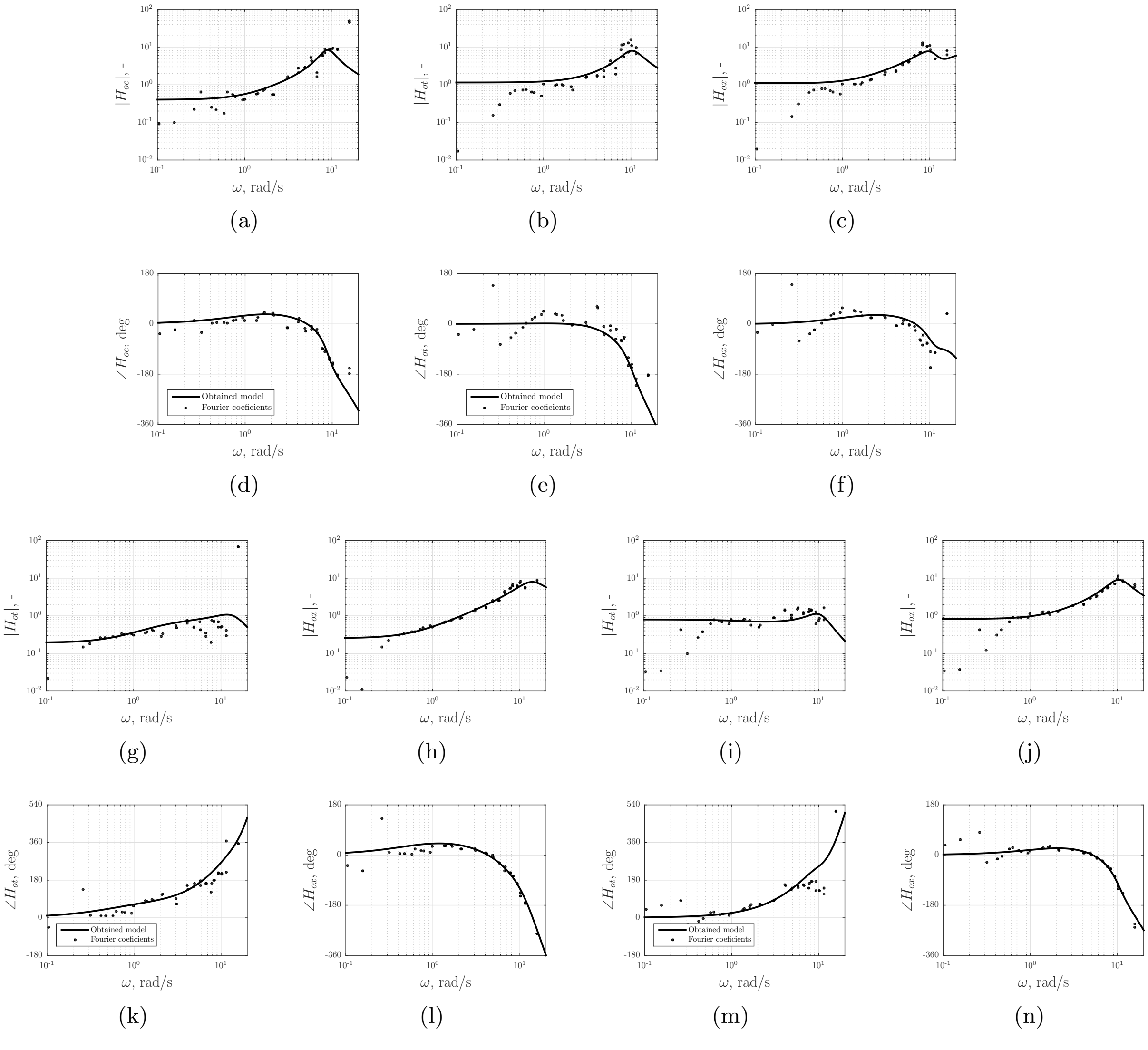

Figure F-1: Human Controller Describing Functions for Subject 1. Results for the compensatory condition without motion feedback (a), (d) and with motion feedback (b), (c), (e), (f) on top and preview without motion feedback (g), (h), (k), (l) and with motion feedback (i), (j), (m), (n)

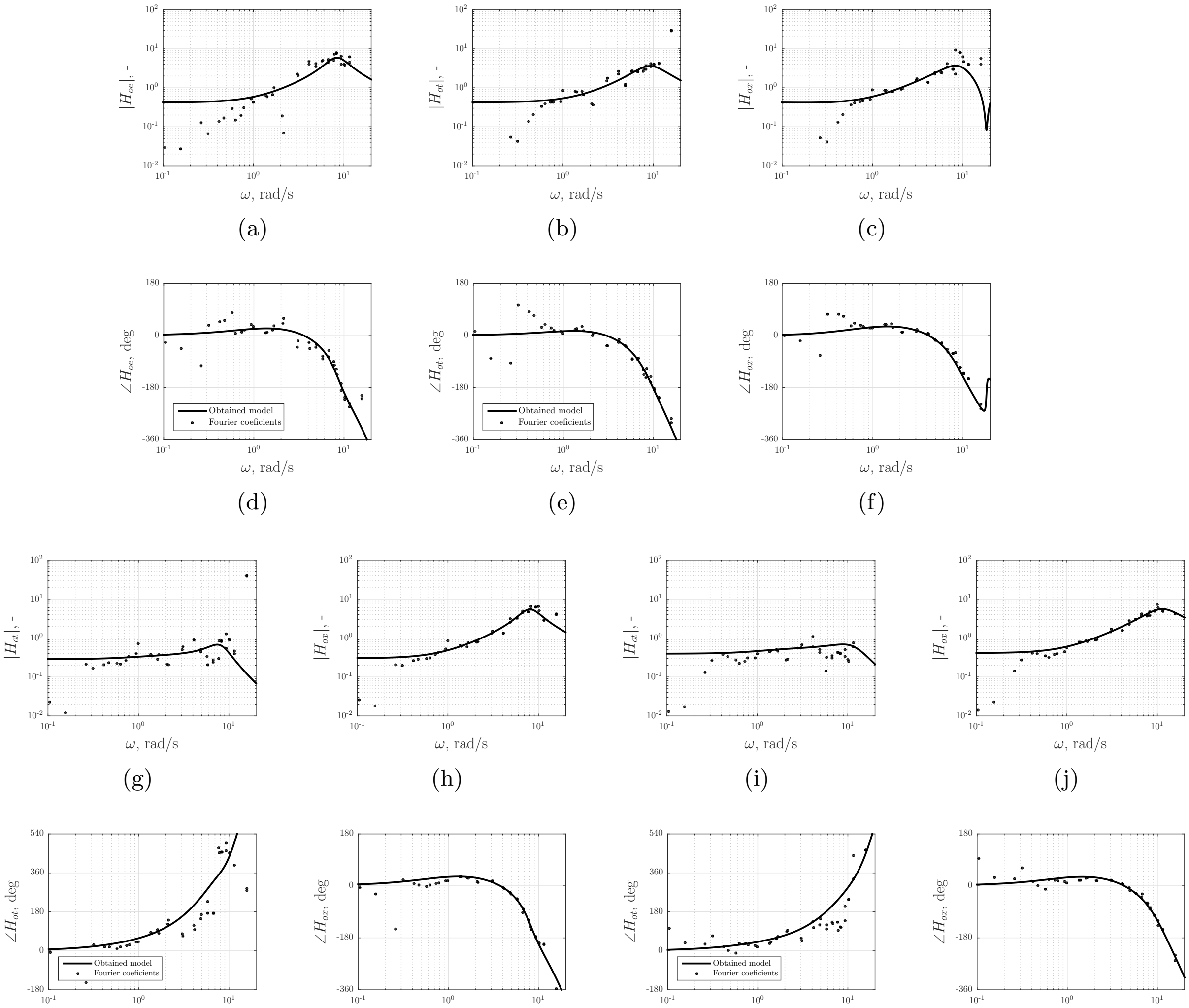

Figure F-2: Human Controller Describing Functions for Subject 2. Results for the compensatory condition without motion feedback (a), (d) and with motion feedback (b), (c), (e), (f) on top and preview without motion feedback (g), (h), (k), (l) and with motion feedback (i), (j), (m), (n)

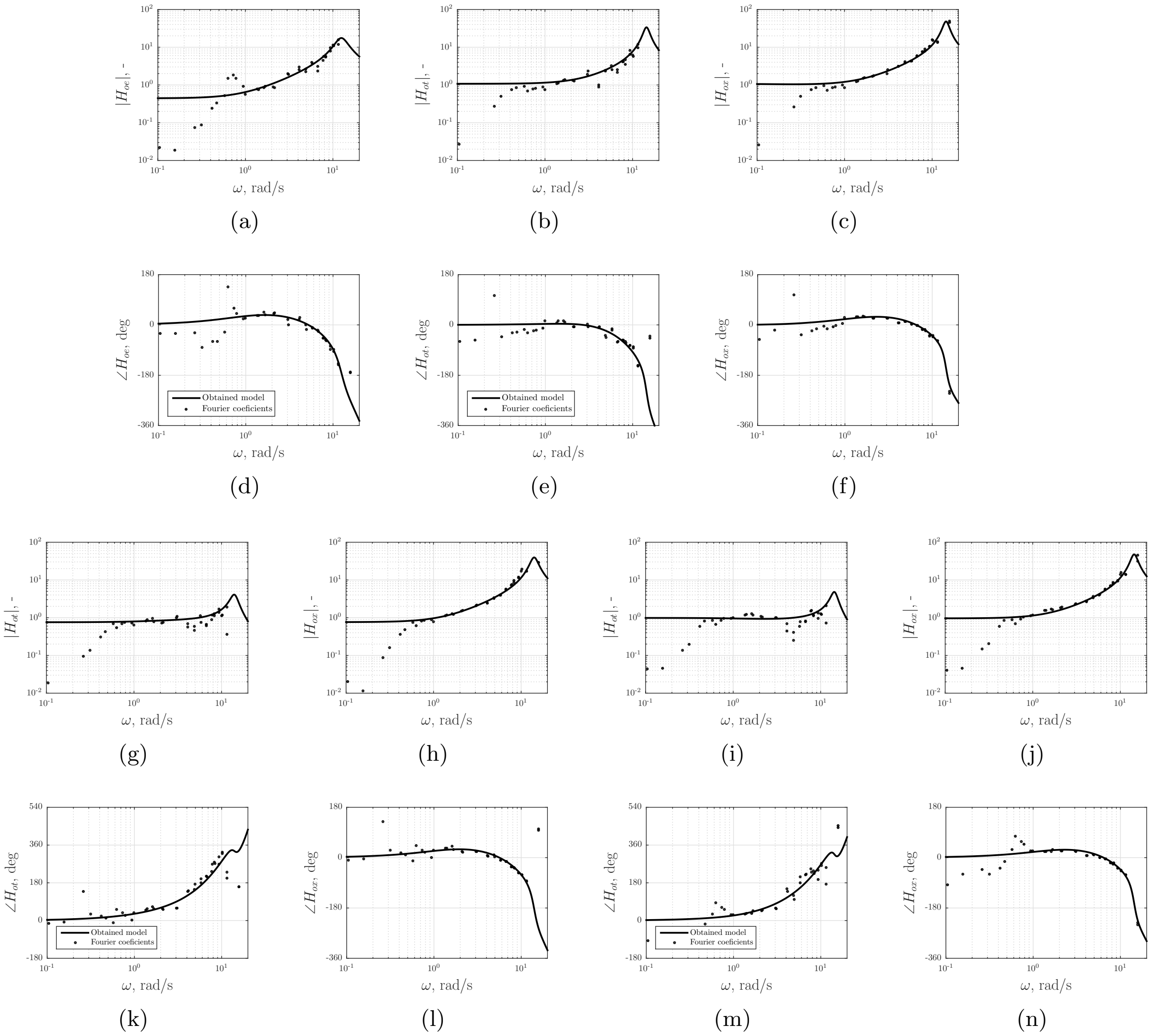

Figure F-3: Human Controller Describing Functions for Subject 3. Results for the compensatory condition without motion feedback (a), (d) and with motion feedback (b), (c), (e), (f) on top and preview without motion feedback (g), (h), (k), (l) and with motion feedback (i), (j), (m), (n)

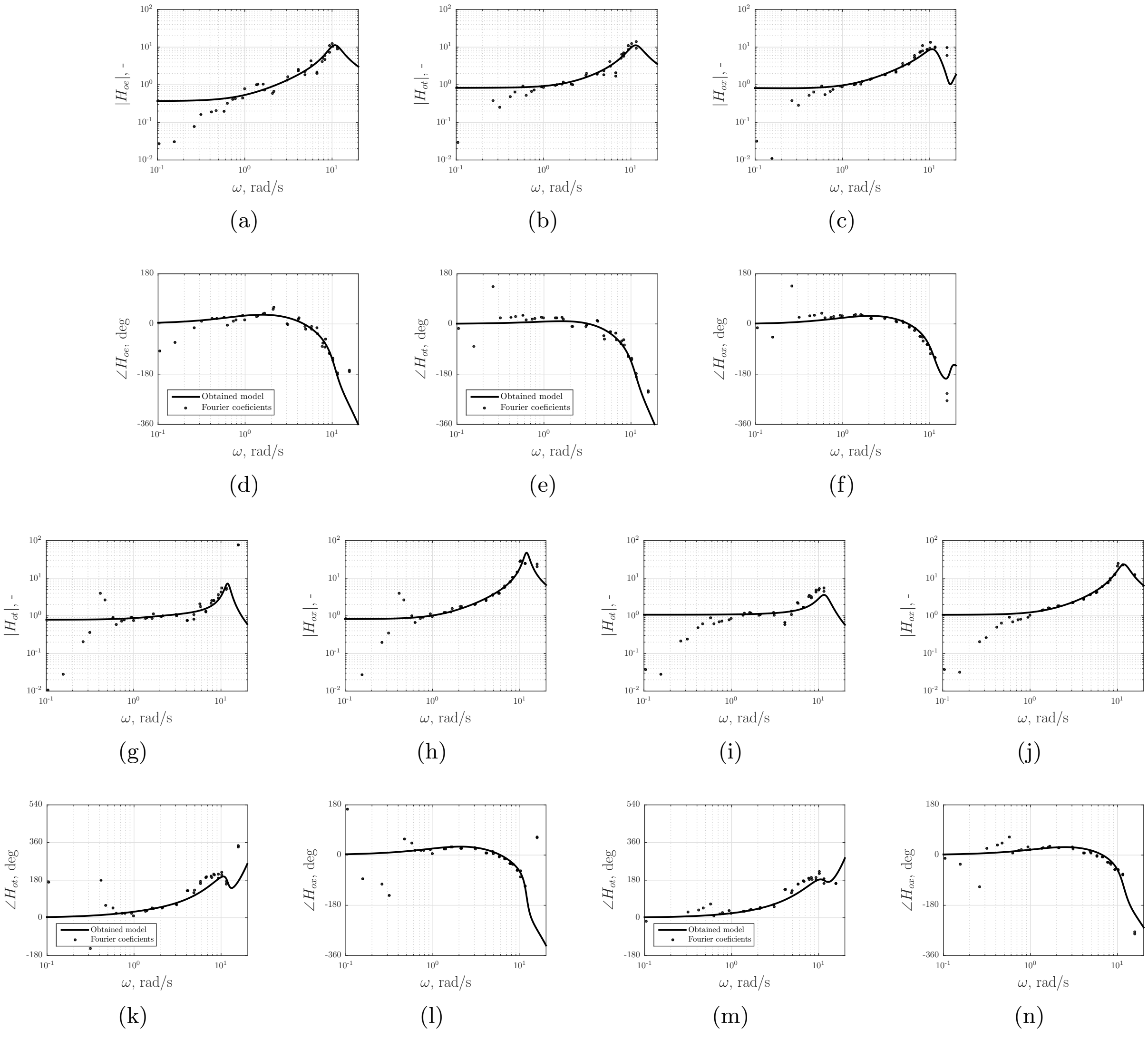

Figure F-4: Human Controller Describing Functions for Subject 4. Results for the compensatory condition without motion feedback (a), (d) and with motion feedback (b), (c), (e), (f) on top and preview without motion feedback (g), (h), (k), (l) and with motion feedback (i), (j), (m), (n)

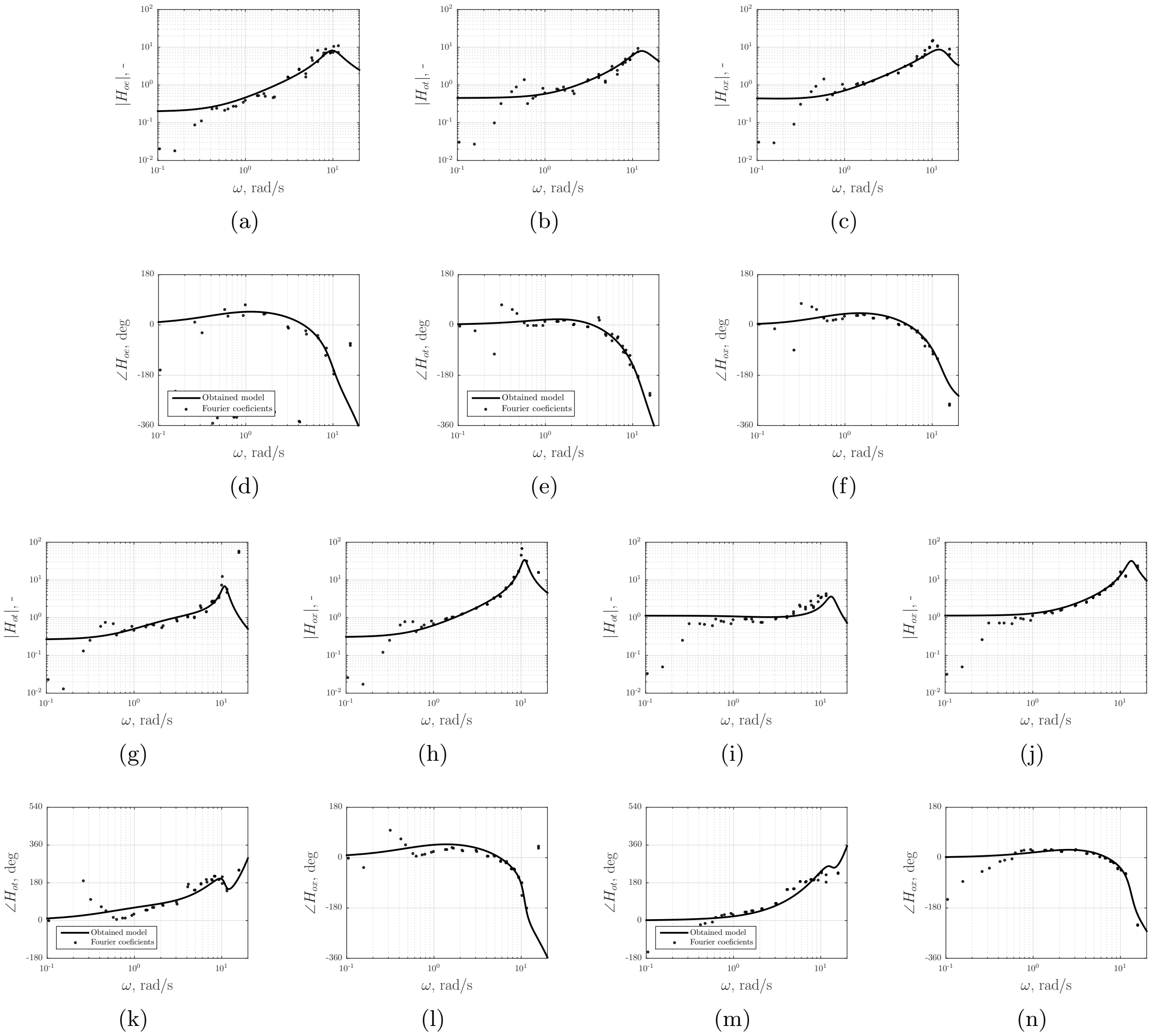

Figure F-5: Human Controller Describing Functions for Subject 5. Results for the compensatory condition without motion feedback (a), (d) and with motion feedback (b), (c), (e), (f) on top and preview without motion feedback (g), (h), (k), (l) and with motion feedback (i), (j), (m), (n)

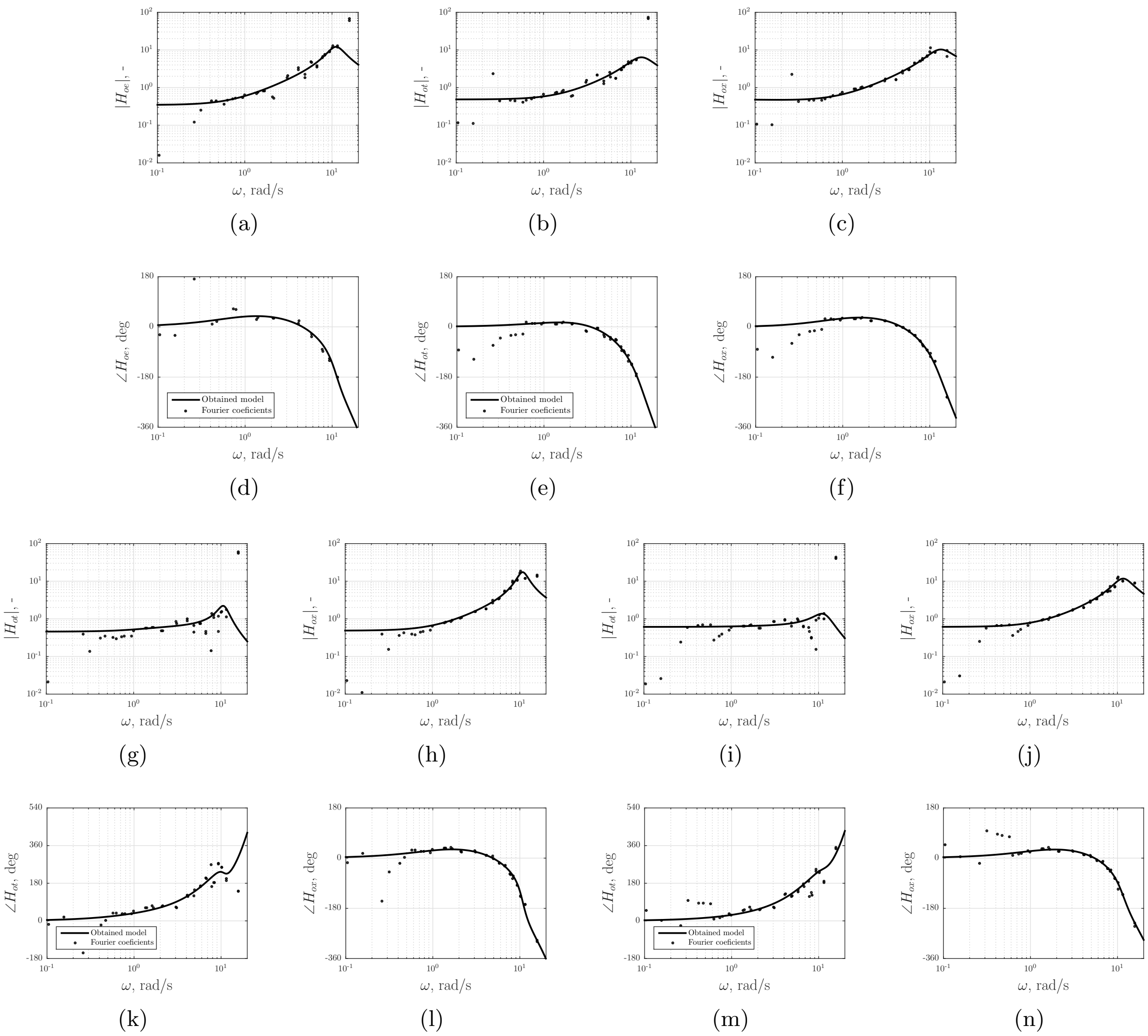

Figure F-6: Human Controller Describing Functions for Subject 6. Results for the compensatory condition without motion feedback (a), (d) and with motion feedback (b), (c), (e), (f) on top and preview without motion feedback (g), (h), (k), (l) and with motion feedback (i), (j), (m), (n)

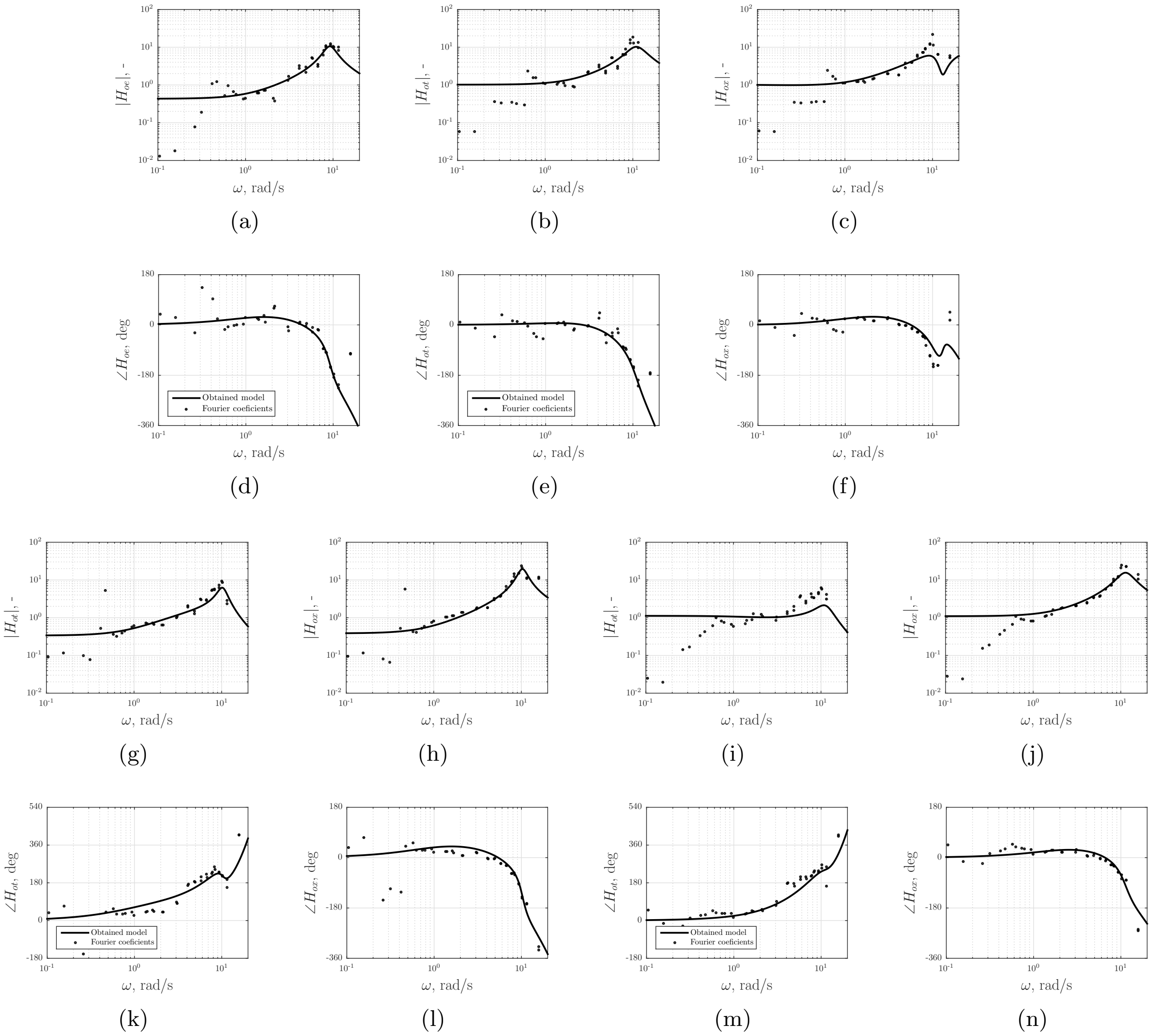

Figure F-7: Human Controller Describing Functions for Subject 7. Results for the compensatory condition without motion feedback (a), (d) and with motion feedback (b), (c), (e), (f) on top and preview without motion feedback (g), (h), (k), (l) and with motion feedback (i), (j), (m), (n)

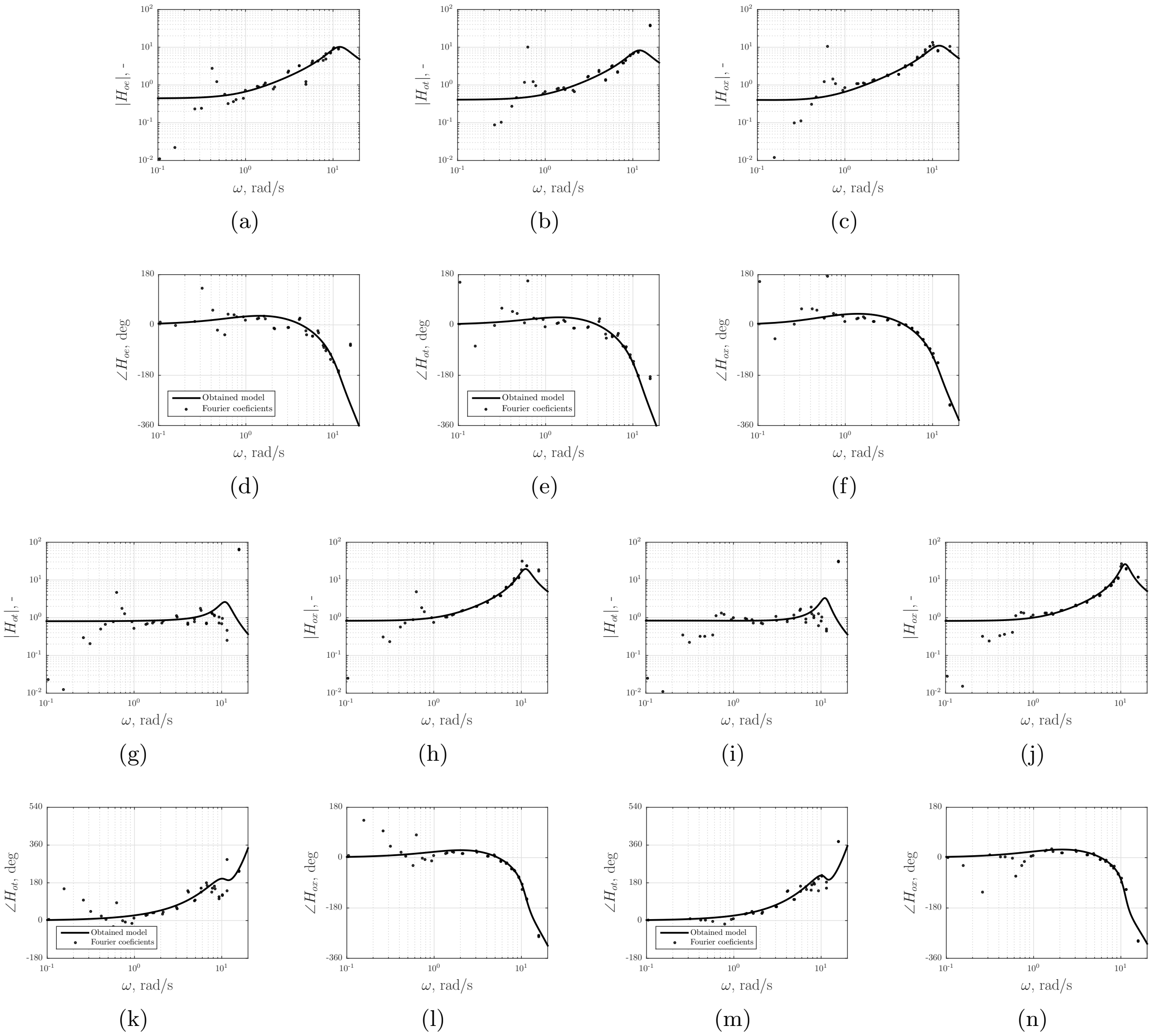

Figure F-8: Human Controller Describing Functions for Subject 8. Results for the compensatory condition without motion feedback (a), (d) and with motion feedback (b), (c), (e), (f) on top and preview without motion feedback (g), (h), (k), (l) and with motion feedback (i), (j), (m), (n)

Appendix G

Estimated Model Parameters

The model parameters were estimated for each subject, for the average in the frequency domain of five measurement runs. 100 optimization runs, each starting with a different parameter set, were conducted. In the following tables, the full results for the parameter estimation are presented, for each of the four experimental conditions and for the eight test subjects.

Table G-1: Parameters for the compensatory task

Subject	$K_e, -$	$T_{L,e}, s$	$\omega_{nms}, rad/s$	$\zeta_{nms}, -$	τ_v, s
1	0.401	0.972	8.937	0.208	0.201
2	0.422	0.942	8.400	0.285	0.277
3	0.444	1.057	12.487	0.167	0.235
4	0.368	1.040	10.782	0.184	0.248
5	0.198	2.105	9.804	0.250	0.257
6	0.346	1.397	11.101	0.223	0.263
7	0.433	0.891	9.195	0.169	0.254
8	0.442	1.119	11.934	0.290	0.262

Table G-2: Parameters for the compensatory task with motion feedback

Subject	$K_e, -$	$T_{L,e}, s$	$\omega_{nms}, rad/s$	$\zeta_{nms}, -$	τ_v, s	$K_m, -$	τ_m, s
1	1.146	0.359	10.343	0.276	0.260	0.438	0.118
2	0.426	0.751	9.192	0.410	0.288	0.149	0.176
3	1.076	0.368	14.429	0.086	0.277	0.350	0.210
4	0.825	0.483	11.327	0.206	0.267	0.225	0.152
5	0.452	0.809	12.767	0.295	0.306	0.264	0.213
6	0.485	0.660	13.221	0.333	0.283	0.188	0.261
7	1.019	0.466	10.997	0.259	0.284	0.331	0.130
8	0.406	0.975	11.973	0.288	0.282	0.158	0.252

Table G-3: Parameters for the preview task

Subject	$K_e, -$	$T_{L,e}, s$	$\omega_{nms}, rad/s$	$\zeta_{nms}, -$	τ_v, s	$K_f, -$	$T_{L,f}, s$	τ_f, s
1	0.255	1.747	13.872	0.389	0.275	0.763	0.433	0.805
2	0.303	1.233	8.092	0.279	0.276	0.946	0.969	1.250
3	0.764	0.770	14.082	0.105	0.221	0.994	0.682	0.742
4	0.820	0.731	11.966	0.076	0.208	0.963	0.525	0.581
5	0.306	1.769	10.915	0.087	0.239	0.866	0.385	0.643
6	0.487	0.938	10.791	0.143	0.245	0.942	0.684	0.758
7	0.385	1.247	10.295	0.127	0.229	0.876	0.249	0.711
8	0.827	0.680	11.172	0.163	0.205	0.977	0.656	0.650

Table G-4: Parameters for the preview task with motion feedback

Subject	$K_e, -$	$T_{L,e}, s$	$\omega_{nms}, rad/s$	$\zeta_{nms}, -$	τ_v, s	$K_f, -$	$T_{L,f}, s$	τ_f, s
1	0.823	0.614	10.397	0.293	0.172	0.971	0.780	0.749
2	0.411	1.060	11.410	0.452	0.228	0.962	0.754	0.863
3	0.961	0.626	14.394	0.092	0.191	1.026	0.705	0.682
4	1.067	0.574	11.841	0.157	0.158	1.006	0.551	0.549
5	1.135	0.553	13.363	0.132	0.162	0.997	0.658	0.614
6	0.612	0.802	11.652	0.245	0.194	0.999	0.754	0.706
7	1.097	0.552	11.340	0.223	0.141	1.021	0.668	0.657
8	0.820	0.688	11.208	0.122	0.196	1.020	0.719	0.654

Appendix H

Near-Viewpoint Response Analysis

In this section, the effects of the near-viewpoint response for the preview conditions will be analyzed. This section includes the comparison of the frequency response function, parameter estimation results and Variance Accounted For, for the preview conditions with and without motion feedback.

H-1 Proposed Model with Near-Viewpoint Response

The preview model for motion, including the near-viewpoint, is presented in Figure H-1.

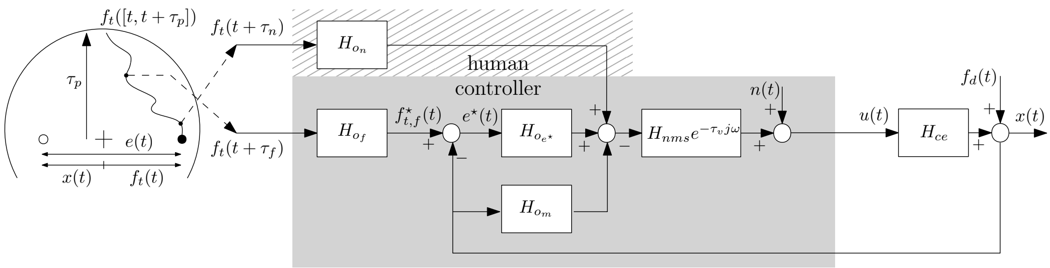

(a)

Figure H-1: Proposed model included near-viewpoint response as in Van der El *et. al*

The near-viewpoint response is modeled as a pure differentiator, as proposed in (El, Pool, Paassen, & Mulder, 2016):

$$H_{o_n} = K_n j\omega \tag{H-1}$$

in which K_n stands for the near-viewpoint gain. The use of this model includes two extra parameters to estimate: the near-viewpoint gain K_n and the near-viewpoint position τ_n.

H-2 Frequency Response Functions

In the Figures 10-2 to 10-9, the frequency response functions of the model with and without near-viewpoint response are presented for all the experiment subjects.

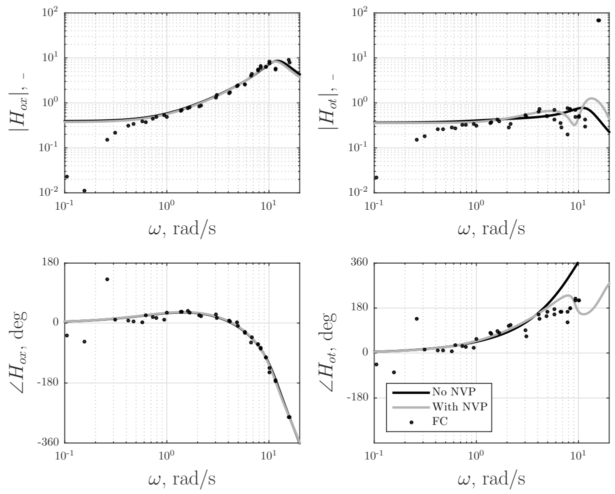

(a)

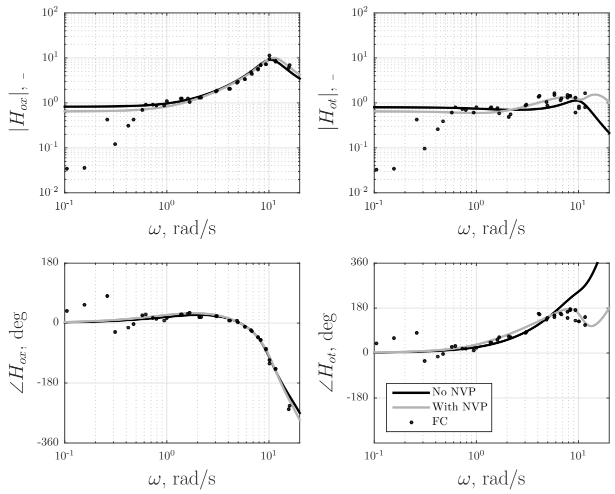

(b)

Figure H-2: Frequency response functions for Subject 1, for the preview condition without motion feedback (a) and with motion feedback (b), with and without the near-viewpoint response

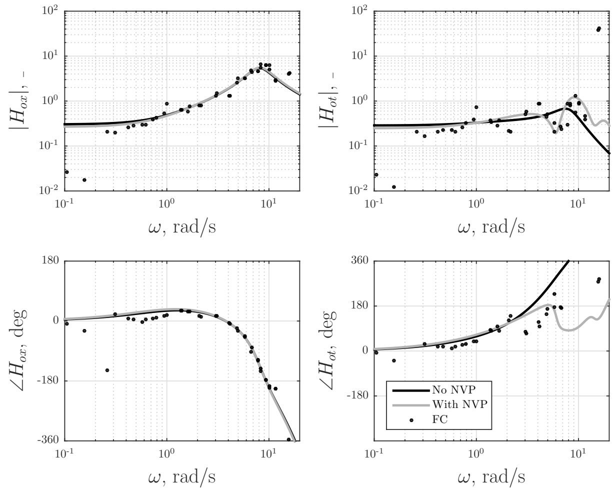

(a)

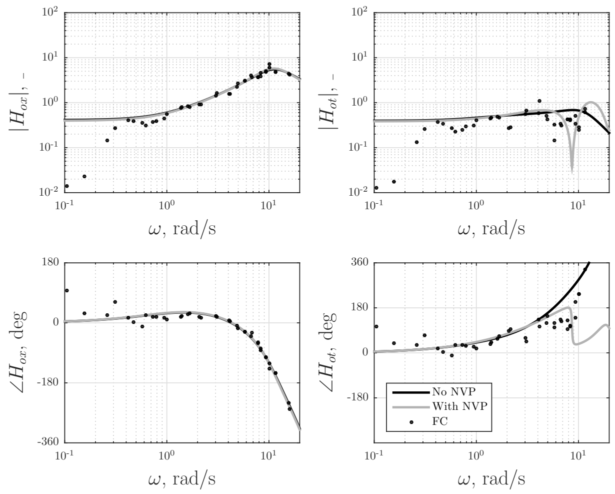

(b)

Figure H-3: Frequency response functions for Subject 2, for the preview condition without motion feedback (a) and with motion feedback (b), with and without the near-viewpoint response

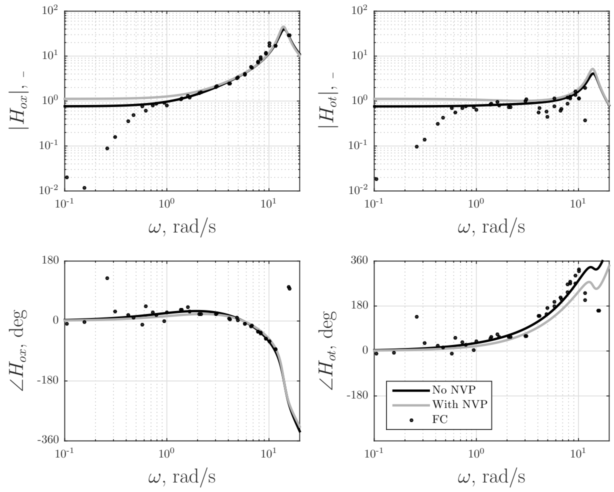

(a)

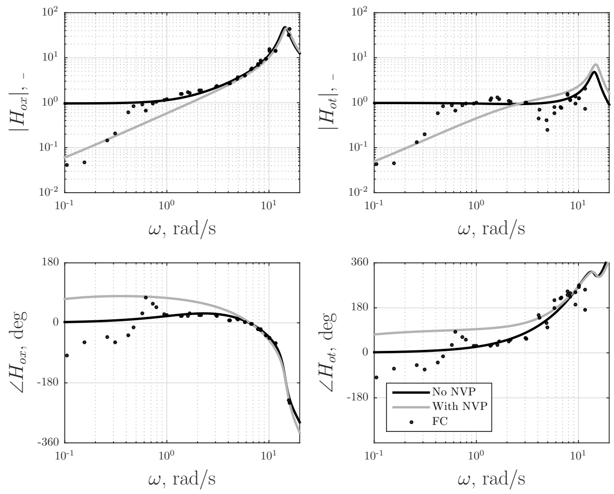

(b)

Figure H-4: Frequency response functions for Subject 3, for the preview condition without motion feedback (a) and with motion feedback (b), with and without the near-viewpoint response

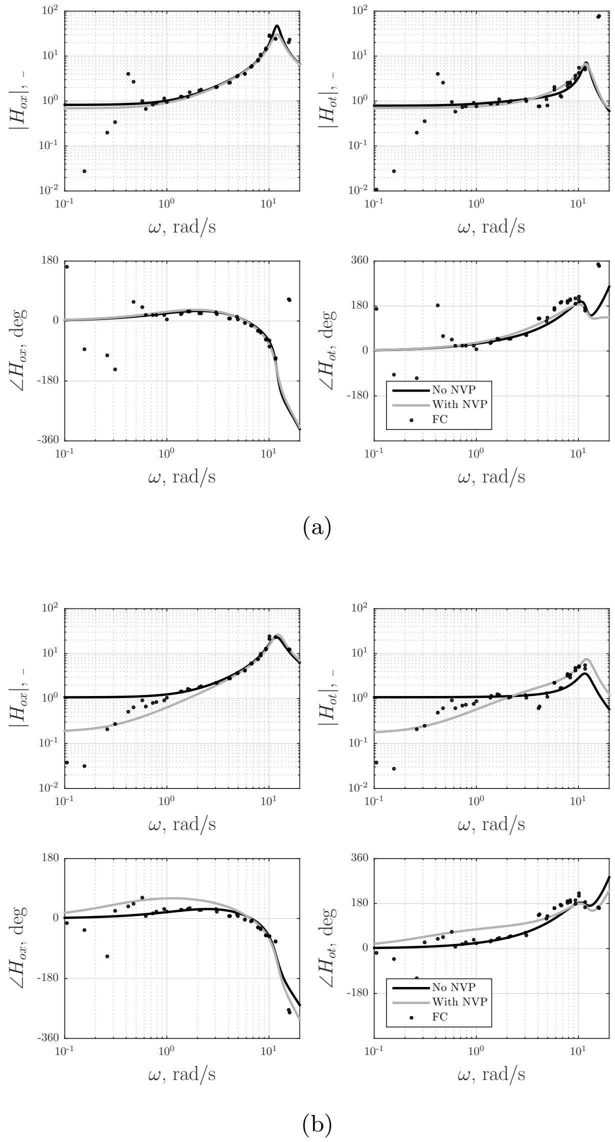

Figure H-5: Frequency response functions for Subject 4, for the preview condition without motion feedback (a) and with motion feedback (b), with and without the near-viewpoint response

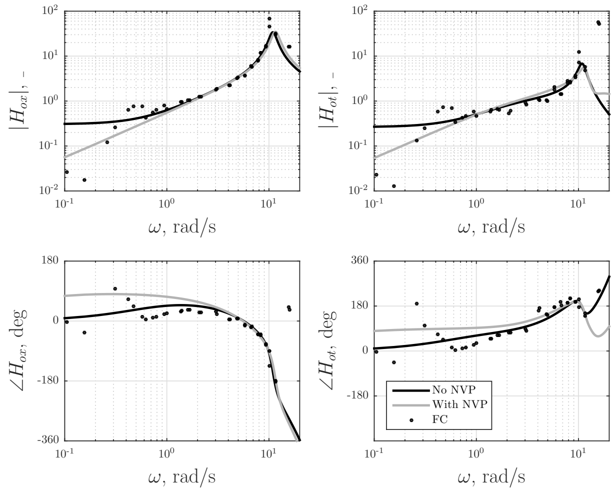

(a)

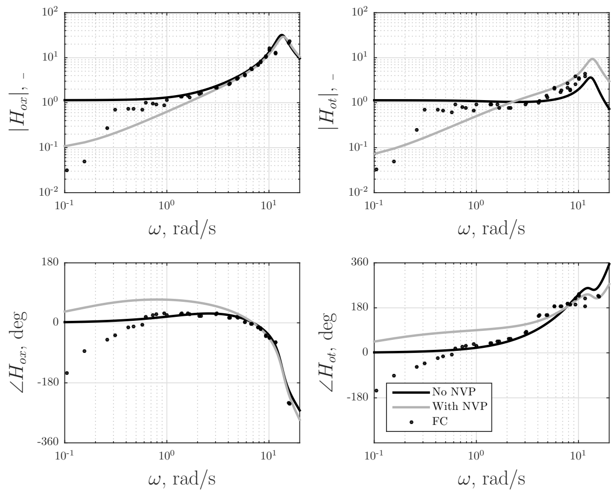

(b)

Figure H-6: Frequency response functions for Subject 5, for the preview condition without motion feedback (a) and with motion feedback (b), with and without the near-viewpoint response

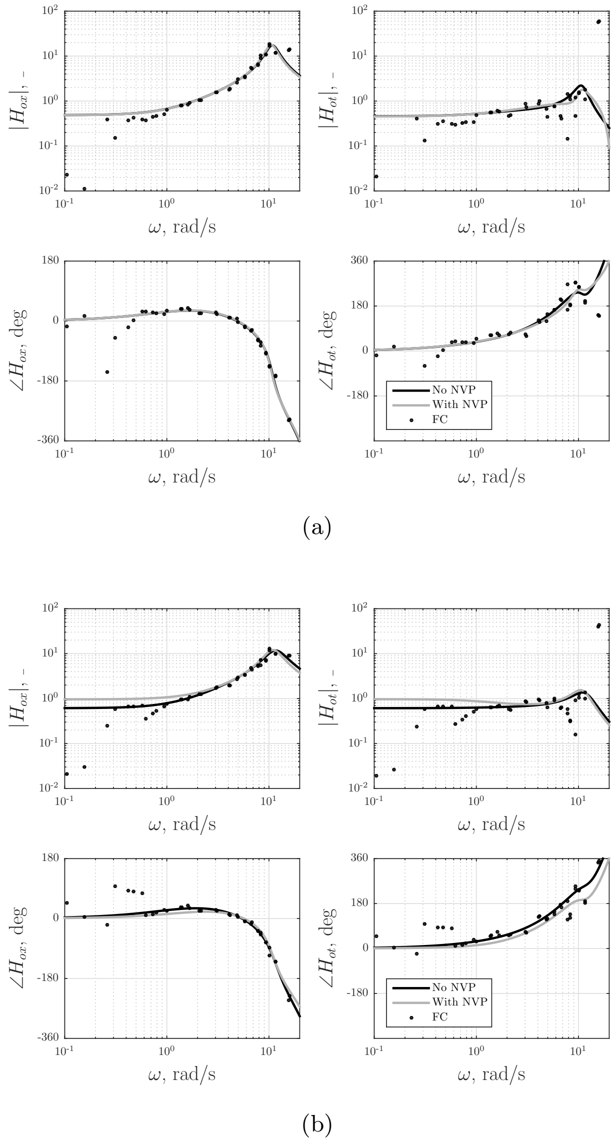

Figure H-7: Frequency response functions for Subject 6, for the preview condition without motion feedback (a) and with motion feedback (b), with and without the near-viewpoint response

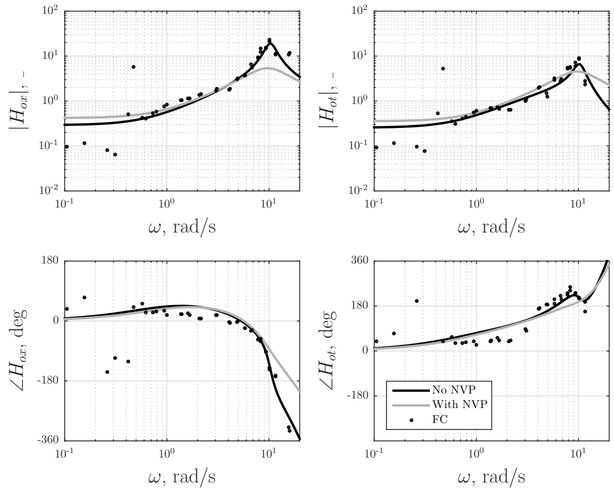

(a)

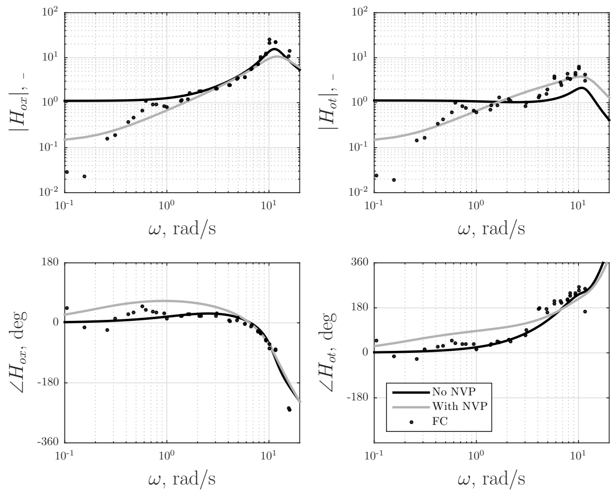

(b)

Figure H-8: Frequency response functions for Subject 7, for the preview condition without motion feedback (a) and with motion feedback (b), with and without the near-viewpoint response

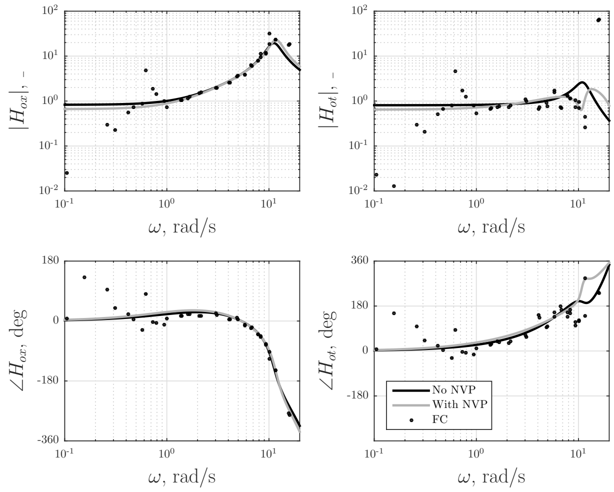

(a)

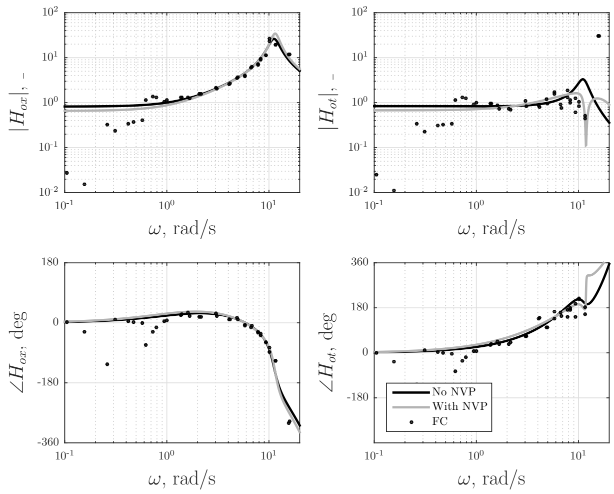

(b)

Figure H-9: Frequency response functions for Subject 8, for the preview condition without motion feedback (a) and with motion feedback (b), with and without the near-viewpoint response

H-3 Parameter Estimation Results

The parameter estimate results including the near-viewpoint response are presented in the following tables.

Table H-1: Parameters for the preview task

Subject	$K_e, -$	$T_{L,e}, s$	$\omega_{nms}, rad/s$	$\zeta_{nms}, -$	τ_v, s	$K_n, -$	τ_n, s	$K_f, -$	$T_{L,f}, s$	τ_f, s
1	0.226	2.048	15.215	0.436	0.290	0.000	0.896	0.894	0.696	0.963
2	0.276	1.365	7.997	0.270	0.278	0.065	0.522	0.935	1.234	1.274
3	0.769	0.764	14.077	0.100	0.221	0.031	0.314	1.000	0.737	0.748
4	0.106	5.787	12.349	0.093	0.235	0.000	0.508	0.914	0.336	0.572
5	0.174	3.021	10.898	0.084	0.247	0.031	0.621	0.751	0.326	0.621
6	0.476	0.951	10.705	0.137	0.244	0.022	0.332	0.945	0.740	0.773
7	0.064	6.986	10.467	0.214	0.250	0.172	0.483	0.567	0.000	0.648
8	0.734	0.780	11.569	0.144	0.217	0.066	0.270	0.987	0.791	0.695

Table H-2: Parameters for the preview task with motion feedback

Subject	$K_e, -$	$T_{L,e}, s$	$\omega_{nms}, rad/s$	$\zeta_{nms}, -$	τ_v, s	$K_n, -$	τ_n, s	$K_f, -$	$T_{L,f}, s$	τ_f, s	$K_m, -$	τ_m, s
1	0.740	0.413	11.533	0.325	0.153	0.120	0.365	0.969	0.836	0.833	0.176	0.328
2	0.586	0.000	9.053	0.658	0.002	0.080	0.321	0.883	0.000	0.577	0.374	0.244
3	0.924	0.622	14.428	0.077	0.185	0.130	0.413	0.974	0.603	0.417	0.000	0.294
4	0.156	1.470	12.132	0.270	0.136	0.323	0.376	0.625	0.271	0.396	0.300	0.292
5	0.076	0.787	13.733	0.249	0.000	0.335	0.261	0.184	0.000	0.261	0.397	0.277
6	0.146	3.577	13.402	0.365	0.216	0.016	0.000	0.940	0.422	0.627	0.021	0.490
7	0.582	0.000	29.704	1.852	0.352	0.334	0.670	0.921	0.404	1.272	0.818	0.236
8	1.308	0.130	12.151	0.204	0.051	0.000	0.249	0.959	0.193	0.429	0.324	0.319

H-4 Variance Accounted For

The Variance Accounted For is a measure of the quality of the model fit. If including the near-viewpoint response lead to a substantial increase in the VAF of the model, there would be a reason to include it in the final model. The results of the VAF per subject are presented in Figure H-10.

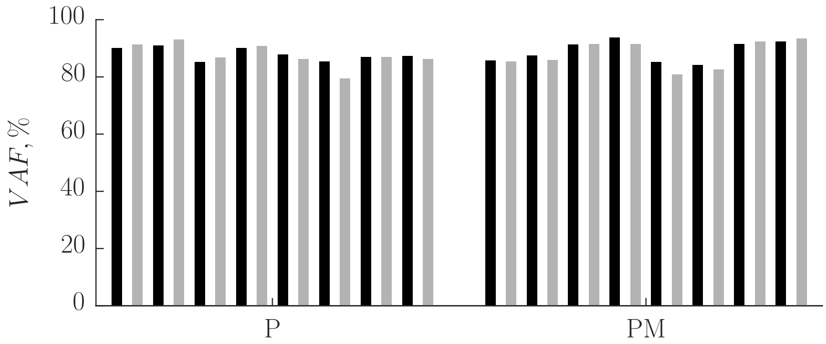

Figure H-10: Variance Accounted For with (grey) and without (black) near-viewpoint

H-5 Model Comparison

For most subjects, there are no substantial changes in the describing function using the near-viewpoint response. The model without near-viewpoint is able to successfully model the response. It should be noted that the obtained parameters are different from the parameter estimates without using a near-viewpoint. The introduction of two extra parameters to estimate leads to a larger estimation uncertainty in the remaining parameters. It is also clear that the near-viewpoint gain K_n, for most subjects, has a small value. Regarding the Variance Accounted For, no significant difference is found using the near-viewpoint response.

Considering these facts, it was decided not to include the near-viewpoint response in the proposed model, to be presented in the paper.

Appendix I

Model Comparison for the Preview Task with Motion Feedback

In this section, the results for the preview task with motion feedback are presented, using both the proposed model for preview with motion feedback and the van der El *et. al* model, without the motion feedback channel. The frequency response functions, parameter estimates and Variance Accounted For are presented for the eight experiment subjects, for both models.

I-1 Frequency Response Functions

The frequency response functions for the eight experiment subjects are presented in the following figures. In each image, the two Bode diagrams of the describing functions H_{o_t} and H_{o_x} are presented. The grey lines present the proposed model fit, the black lines the van der El *et. al* model fit, and the black dots the Fourier coefficients.

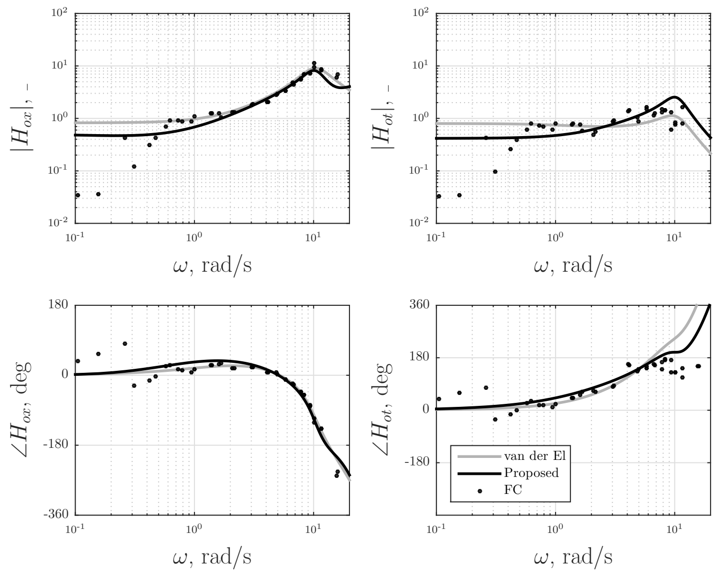

(a)

Figure I-1: Frequency response functions for Subject 1, for the van der El model and the proposed model including motion feedback

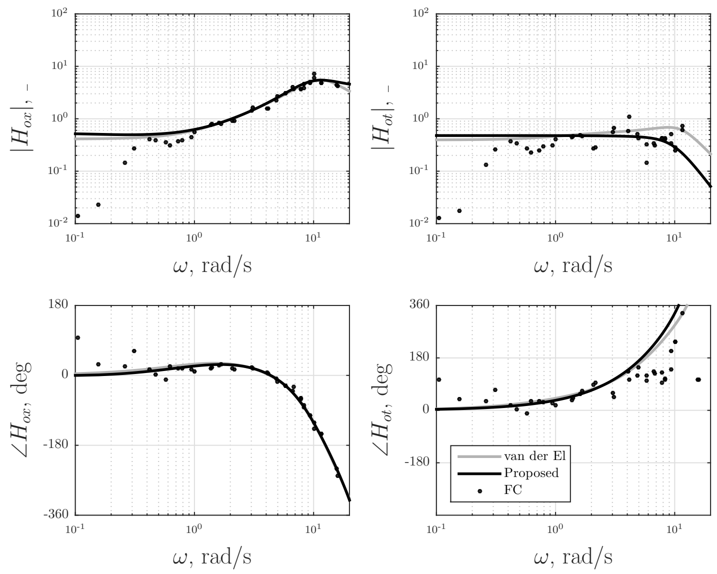

(a)

Figure I-2: Frequency response functions for Subject 2, for the van der El model and the proposed model including motion feedback

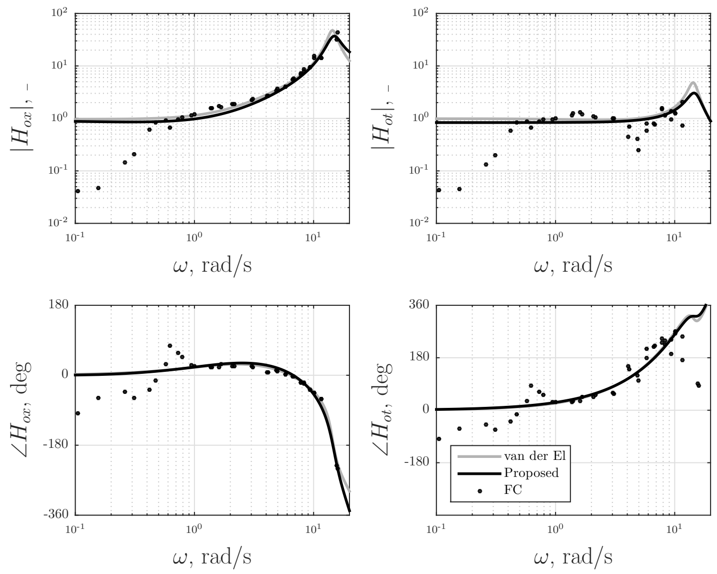

(a)

Figure I-3: Frequency response functions for Subject 3, for the van der El model and the proposed model including motion feedback

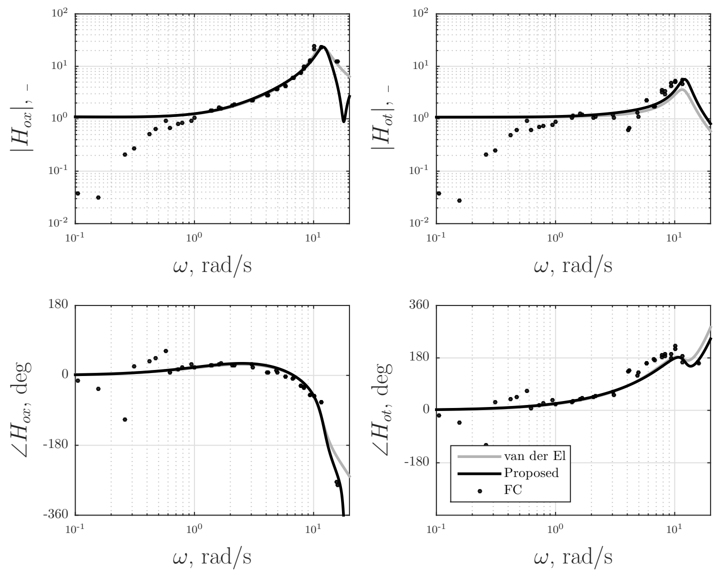

(a)

Figure I-4: Frequency response functions for Subject 4, for the van der El model and the proposed model including motion feedback

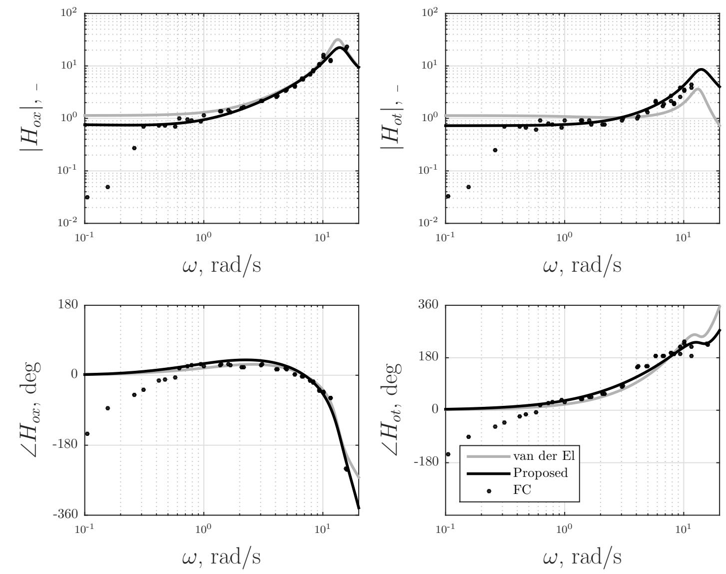

(a)

Figure I-5: Frequency response functions for Subject 5, for the van der El model and the proposed model including motion feedback

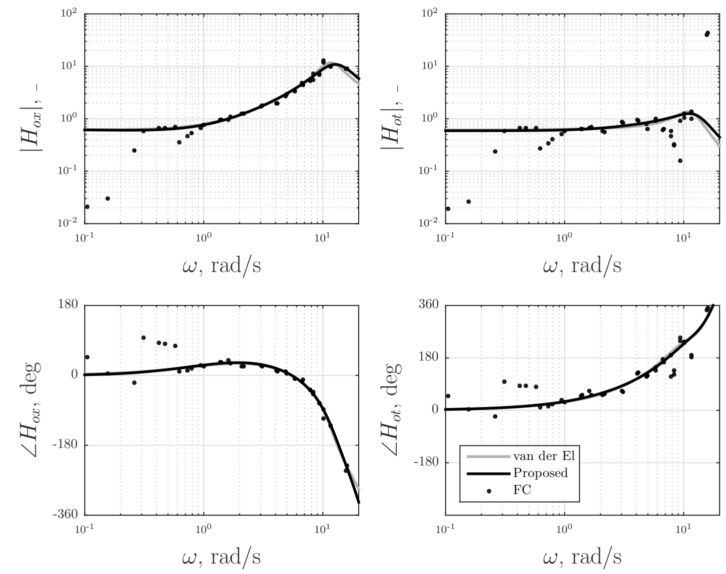

(a)

Figure I-6: Frequency response functions for Subject 6, for the van der El model and the proposed model including motion feedback

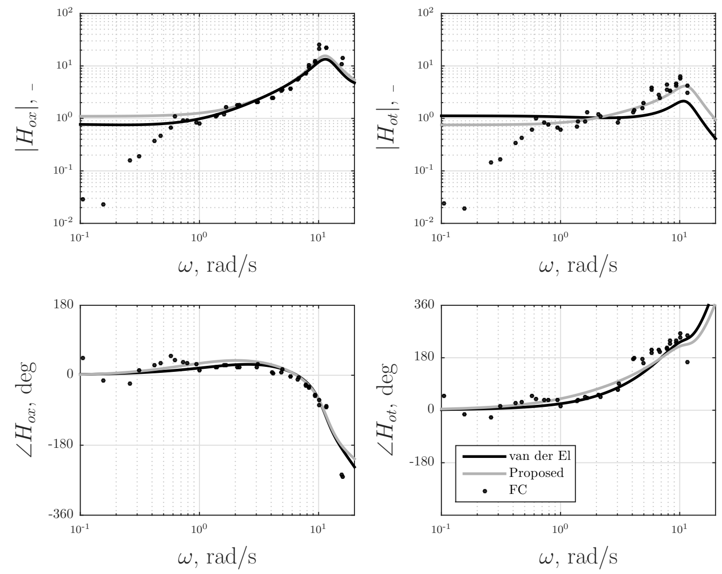

(a)

Figure I-7: Frequency response functions for Subject 7, for the van der El model and the proposed model including motion feedback

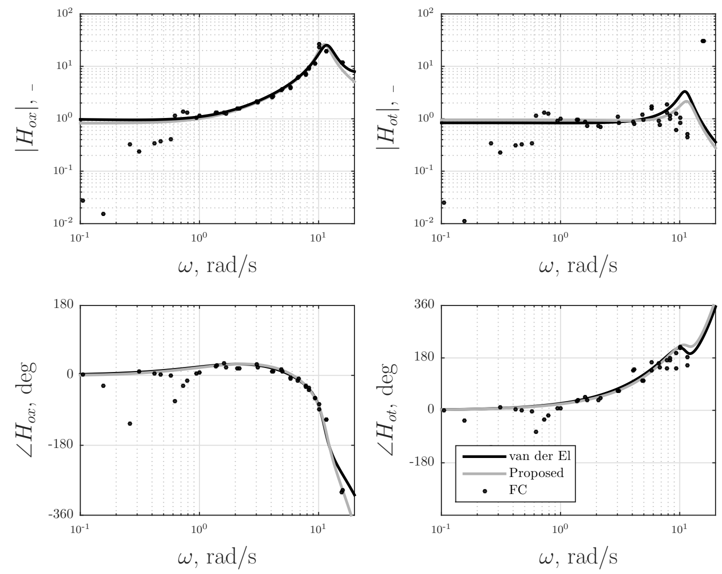

(a)

Figure I-8: Frequency response functions for Subject 8, for the van der El model and the proposed model including motion feedback

I-2 Model Parameters

The model parameters are presented in the following tables, for the van der El *et. al* model and the proposed model.

Table I-1: Parameters for the preview task with motion feedback using the proposed model

Subject	$K_e, -$	$T_{L,e}, s$	$\omega_{nms}, rad/s$	$\zeta_{nms}, -$	τ_v, s	$K_f, -$	$T_{L,f}, s$	τ_f, s
1	0.574	0.547	11.857	0.442	0.158	0.899	0.196	0.622
2	0.522	0.071	10.032	0.593	0.173	0.892	0.001	0.829
3	1.110	0.017	14.251	0.122	0.009	0.940	0.000	0.377
4	0.420	1.285	11.965	0.125	0.232	0.977	0.263	0.573
5	0.971	0.323	14.621	0.104	0.102	0.934	0.177	0.500
6	0.591	0.331	12.614	0.399	0.137	0.945	0.162	0.602
7	0.719	0.589	15.164	0.119	0.144	0.968	0.166	0.535
8	0.973	0.013	11.679	0.136	0.000	0.956	0.151	0.547

Table I-2: Parameters for the preview task with motion feedback using the van der El model

Subject	$K_e, -$	$T_{L,e}, s$	$\omega_{nms}, rad/s$	$\zeta_{nms}, -$	τ_v, s	$K_f, -$	$T_{L,f}, s$	τ_f, s
1	0.574	0.547	11.857	0.442	0.158	0.899	0.196	0.622
2	0.522	0.071	10.032	0.593	0.173	0.892	0.001	0.829
3	1.110	0.017	14.251	0.122	0.009	0.940	0.000	0.377
4	0.420	1.285	11.965	0.125	0.232	0.977	0.263	0.573
5	0.971	0.323	14.621	0.104	0.102	0.934	0.177	0.500
6	0.591	0.331	12.614	0.399	0.137	0.945	0.162	0.602
7	0.719	0.589	15.164	0.119	0.144	0.968	0.166	0.535
8	0.973	0.013	11.679	0.136	0.000	0.956	0.151	0.547

I-3 Variance Accounted For

The Variance Accounted For is presented in Figure I-9 for both models.

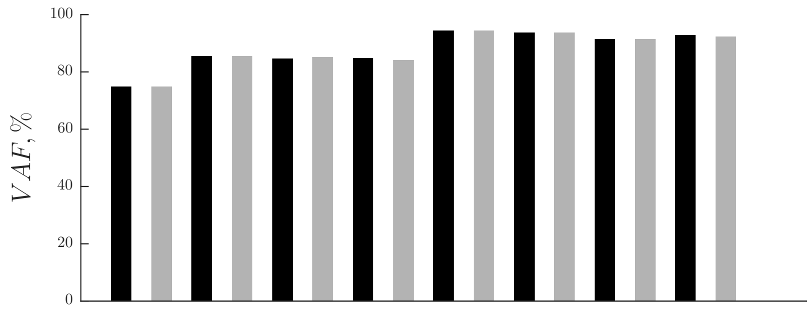

Figure I-9: Variance Accounted For for the proposed model (black) and van der El *et al* model (grey)

I-4 Model Comparison

When analyzing the describing functions, it is clear that the visual channel from the van der El *et. al* model is able to model the response. The additional motion feedback channel in the proposed model doesn't make a substantial difference in the resulting describing function. There is a change in some of the parameters when using the van der El *et. al* model, most notably the lead-time constant $T_{L,e}$, the time delay τ_v and the far-viewpoint time constant $T_{l,f}$. No substantial difference is found in the Variance Accounted For of the models.

Appendix J

Offline Model Simulations with Human Adaptation

Offline model simulations were performed in order to predict and validate the results of the experiment. The offline model simulation were performed using the model in Figure J-1.

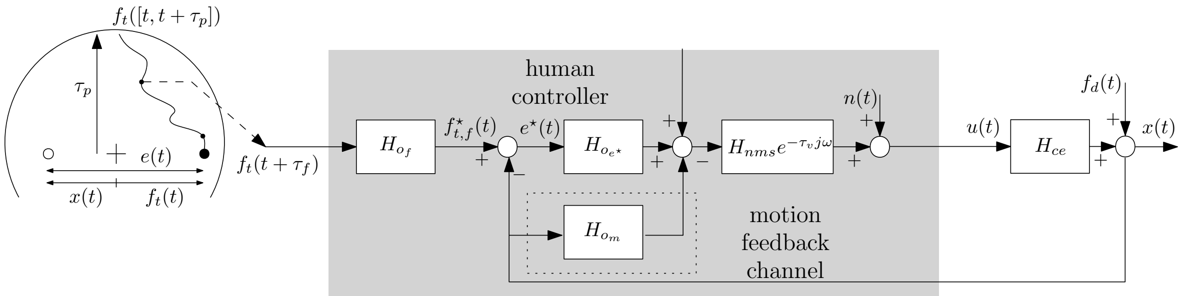

Figure J-1: Proposed preview model

In literature on compensatory tasks with motion feedback, it is shown that motion has a substantial effect on the parameters of the human model (Lu et al., 2015; Pool, Damveld, Paassen, & Mulder, 2011). In (Pool et al., 2011), equations were derived for the changes in different motion cueing settings. The two main adaptations of the human controller for the compensatory case are:

$$K_e(0) = K_e(1)[0.19(K_S - 1) + 1] \tag{J-1}$$

$$T_{L,e}(0) = T_L(1)[-0.29(K_S - 1) + 1] \tag{J-2}$$

In these equations, K_s is the motion filter gain. For the present case, $K_s = 0$ is the no motion condition, and $K_s = 1$ the motion condition. In an attempt to consider these changes in the offline model simulations, four simulation conditions were defined: compensatory (C), preview

(P), compensatory with human adaptation (CA) and preview with human adaptation (PA). The last condition was defined under the hypothesis that the human controller may show the same kind of adaptation in preview tasks as was previously found in compensatory tasks.

J-1 Model Settings

The model settings for the simulations are presented in Table J-1. Double integrator dynamics were used for the controlled element, given by $5/(j\omega)^2$. The compensatory parameters are obtained from the results of (Lu et al., 2015) and the preview parameters are based on the results of (El et al., 2015).

Table J-1: Parameters for offline model simulations

Conditions	$K_{e^\star}, -$	$T_{L,e^\star}, s$	$\omega_{nms}, rad/s$	$\zeta_{nms}, -$
C	0.20	1.70	12	0.40
CA	0.25	1.32	12	0.40
P	0.20	2	6	0.45
PA	0.25	1.55	6	0.45
	τ_v, s	$K_f, -$	$T_{L,f}, s$	τ_f, s
C	0.30	1	0	0
C	0.30	1	0	0
P	0.30	0.9	1	1
PA	0.30	0.9	1	1

J-2 Motion Parameters

Two motion parameters are included in the proposed model: the motion gain K_m and the motion time delay τ_m. In the simulations, K_m was increased from 0 (no motion) to 0.25 in increments of 0.05. The motion time delay is fixed at 0.2, as found in literature (Lu et al., 2015).

J-3 Results

In the following figures, the results of the offline model simulations with adaptation are presented. These results include tracking performance and control activity, crossover frequency and phase margin.

From these results, it can be seen the adaptation doesn't yield substantially different results from the model without adaptation. Even without any change in the human controller parameters, the variance of the error is reduced for the compensatory task, but it is still increased for

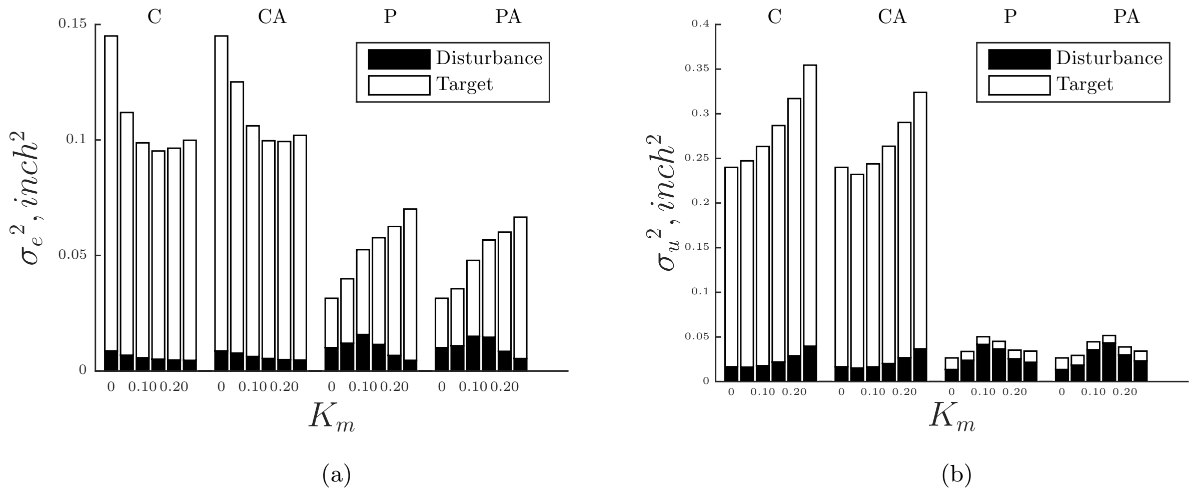

Figure J-2: Variance of the tracking error (a) and control activity (b)

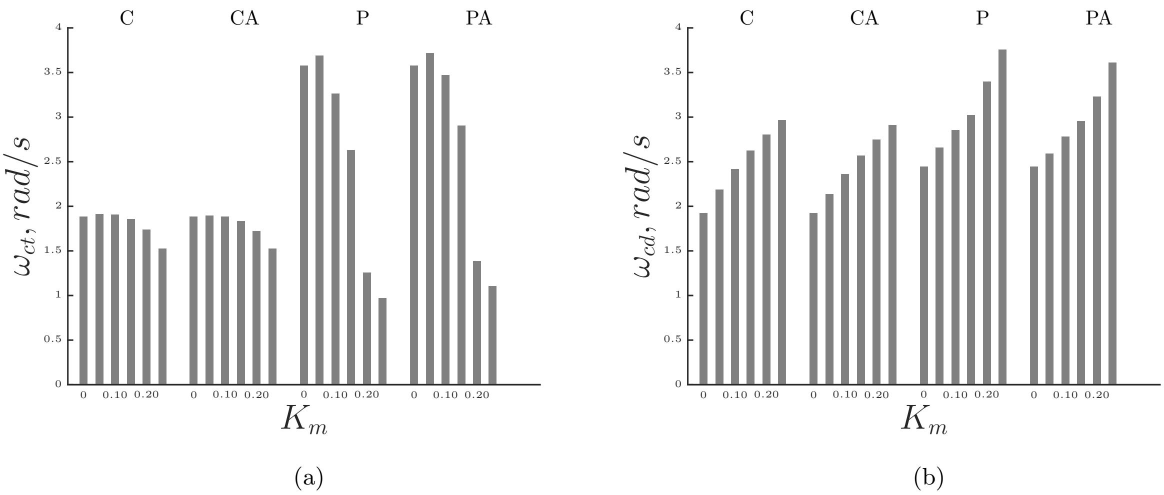

Figure J-3: Target (a) and disturbance (b) crossover frequency

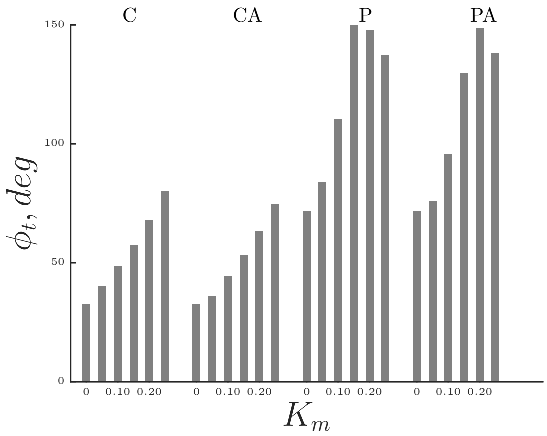

(a)

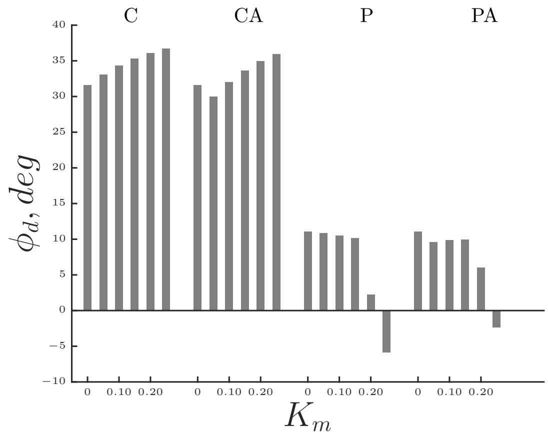

(b)

Figure J-4: Target (a) and disturbance (b) phase margin

the preview task with the adaptation. It should also be noted that the adaptation stabilizes the system up to an higher K_m (0.19 for the condition without adaptation and 0.23 for the condition with adaptation), as can be seen by the smaller gray bar on Figure J-4.

Bibliography

Damveld, H. J., Beerens, G. C., Paassen, M. M. van, & Mulder, M. (2010, July). Design of Forcing Functions for the Identification of Human Control Behavior. *Journal of Guidance, Control, and Dynamics*, *33*(4), 1064-1081.

El, K. van der, Pool, D. M., Damveld, H. J., Paassen, M. M. van, & Mulder, M. (2015). An Empirical Human Controller Model for Preview Tracking Tasks. *IEEE Transactions on Cybernetics*.

El, K. van der, Pool, D. M., Paassen, M. M. van, & Mulder, M. (2016). How Human Controllers use Preview to Improve Target-Tracking Performance. *IEEE Transactions on Cybernetics*.

Guo, K., & Guan, H. (1993). Modelling of Driver/Vehicle Directional Control System. *Vehicle System Dynamics*, *22*(3), 141-184.

Hosman, R. J. A. W. (1996). *Pilot's Perception and Control of Aircraft Motions.* Unpublished doctoral dissertation, Delft University of Technology, Faculty of Aerospace Engineering.

Hosman, R. J. A. W., & Vaart, J. C. van der. (1981). Effects of Vestibular and Visual Motion Perception on Task Performance. *Acta Psychologica*, *48*, 271-287.

Ito, K., & Ito, M. (1975). Tracking behavior of human operators in preview control systems. *Electrical Engineering in Japan*, *95*(1), 120-127.

Jex, H. R., Magdaleno, R. E., & Junker, A. M. (1978). Roll Tracking Effects of G-vector Tilt and Various Types of Motion Washout. In *Proceedings of the fourteenth annual conference on manual control* (p. 463-502).

Lu, T., Pool, D. M., Paassen, M. M. van, & Mulder, M. (2015, September). Use of Simulator Motion Feedback for Different Classes of Vehicle Dynamics in Manual Control Tasks. In *Proceedings of the 5th ceas air & space conference, delft, the netherlands.*

MacAdam, C. C. (2003, January). Understanding and Modeling the Human Driver. *Vehicle System Dynamics*, *40*(1-3), 101-143.

McRuer, D., & Jex, H. (1967). A Review of Quasi-Linear Pilot Models. *IEEE Transactions on Human Factors in Electronics*, *8*(3), 231-249.

Nieuwenhuizen, F. M., Zaal, P. M. T., Mulder, M., Paassen, M. M. van, & Mulder, J. A. (2008, July-August). Modeling Human Multichannel Perception and Control Using

Linear Time-Invariant Models. *Journal of Guidance, Control, and Dynamics*, *31*(4), 999–1013.

Paassen, M. M. van, & Mulder, M. (1998). Identification of Human Operator Control Behaviour in Multiple-Loop Tracking Tasks. In *Proceedings of the seventh ifac/ifip/ifors/iea symposium on analysis, design and evaluation of man-machine systems, kyoto japan* (pp. 515–520). Pergamon.

Padmos, S., El, K. van der, Pool, D. M., Damveld, H. J., Paassen, M. M. van, & Mulder, M. (2016). The effect of preview time on human control behavior in rate and acceleration tracking tasks. *In preparation*.

Pool, D. M. (2012). *Objective Evaluation of Flight Simulator Motion Cueing Fidelity Through a Cybernetic Approach*. Unpublished doctoral dissertation, Delft University of Technology, Faculty of Aerospace Engineering.

Pool, D. M., Damveld, H. J., Paassen, M. M. van, & Mulder, M. (2011). Tuning Models of Pilot Tracking Behavior for a Specific Simulator Motion Cueing Setting. In *Proceedings of the aiaa modeling and simulation technologies conference, portland, oregon, aug. 8-11.*

Pool, D. M., Harder, G. A., & Paassen, M. M. van. (2016). Effects of Simulator Motion Feedback on Training of Skill-Based Control Behavior. *Journal of Guidance, Control, and Dynamics*, *39*(4), 889-902.

Pool, D. M., Mulder, M., Paassen, M. M. van, & Vaart, J. C. van der. (2008). Effects of Peripheral Visual and Physical Motion Cues in Roll-Axis Tracking Tasks. *Journal of Guidance, Control, and Dynamics*, *31*(6), 1608-1622.

Pool, D. M., Valente Pais, A. R., Vroome, A. M. de, Paassen, M. M. van, & Mulder, M. (2012, May–June). Identification of Nonlinear Motion Perception Dynamics Using Time-Domain Pilot Modeling. *Journal of Guidance, Control, and Dynamics*, *35*(3), 749-763.

Repa, B. S., Leucht, P. M., & Wierwille, W. W. (1981, October). The Influence of Motion Cues on Driver-Vehicle Performance in a Simulator. In *Proceedings of the seventeenth annual conference on manual control, los angeles (ca)* (p. 157-169).

Schroeder, J. A. (1993). Simulation Motion Effects on Single Axis Compensatory Tracking. In *Proceedings of the aiaa flight simulation technologies conference, monterey (ca)* (p. 202-213).

Sheridan, T. B. (1966). Three models of preview control. *IEEE Transactions on Human Factors in Electronics*, *7*(2), 91-102.

Tomizuka, M., & Whitney, D. E. (1973). The Preview Control Problem with Application to Man-Machine System Analysis. In *Proceedings of the ninth annual conference on manual control* (p. 429-441).

Vos, M. C., Pool, D. M., Damveld, H. J., Paassen, M. M. van, & Mulder, M. (2014, October). Identification of Multimodal Control Behavior in Pursuit Tracking Tasks. In *Proceedings of the 2014 ieee international conference on systems, man, and cybernetics, san diego (ca)* (p. 69-74).

Zaal, P. M. T., Pool, D. M., Bruin, J. de, Mulder, M., & Paassen, M. M. van. (2009). Use of Pitch and Heave Motion Cues in a Pitch Control Task. *Journal of Guidance, Control, and Dynamics*, *32*(2), 366-377.

Zaal, P. M. T., Pool, D. M., Chu, Q. P., Paassen, M. M. van, Mulder, M., & Mulder, J. A. (2009). Modeling Human Multimodal Perception and Control Using Genetic Maximum Likelihood Estimation. *Journal of Guidance, Control, and Dynamics*, *32*(4), 1089-1099.